

PACKING STRUCTURE OF POWDER COMPACTS

Aidana Boribayeva, B. Sc. in Chemistry

**Submitted in fulfillment of the requirements for the degree of
Master of Science in Chemical and Materials Engineering**



**School of Engineering and Digital Sciences
Department of Chemical and Materials Engineering
Nazarbayev University**

53 Kabanbay Batyr Avenue,
Nur-Sultan, Kazakhstan, 010000

Supervisor: Dr. Boris Golman

Co-supervisor: Dr. Assiya Yermukhambetova

April 2021

Declaration

I hereby, declare that this manuscript, entitled “Packing structure of powder compacts”, is the result of my own work except for quotations and citations which have been duly acknowledged.

I also declare that, to the best of my knowledge and belief, it has not been previously or concurrently submitted, in whole or in part, for any other degree or diploma at Nazarbayev University or any other national or international institution.



Name: Aidana Boribayeva

Date: 11 April 2021

Abstract

The particle packing process is the major step in manufacturing of high-performance products and materials production in many industries. The shape and size of particles are the most important factors influencing the packing process. Therefore, in the recent years, there has been a growing interest in the investigation of packing structure of powder compacts containing non-spherically shaped particles. However, the thorough analysis of compact morphology is still limited. Thus, the main aim of the thesis work is to study the effects of various shapes of non-spherical particles and addition of non-spherical particles into spherical particles mixture on the packing microstructure of obtained compacts.

The thesis reviews methodologies currently applied in the evaluation of packed compacts characteristics such as discrete element method, void size distribution and Voronoi tessellation analyses. Initial steps of creation of packed powder compacts employed DEM with superquadrics approach to generate non-spherical shaped particles. The provided two studies covered different simulation objects. The first samples are three specimens: pills, cylinders, and spheres of 45,000 particles in each compact with similar particles volume in order to focus on the packing structure analysis of shape effect. The second samples are four specimens of binary mixture of spheres ($r_{fine}:r_{coarse}$ 2cm: 4cm) with and without inclusion of fibers: $f_{fine}:f_{coarse}:f_{fiber}$ 63:37:0, 62:37:1, 40:60:0, and 40:59:1.

The results of first study analysis showed a trend of void size distribution among cross-sectional images normal to x and y with the dominance of small voids and uniform voids distribution for pills and cylinders compacts. However, symmetrical shape of spherical particles compacts affected to the small voids distribution in z direction in comparison with other two samples. Furthermore, the characteristics of constructed Voronoi diagram depicted voronoi cells volumes and surface areas. The pills compact showed the highest peak with narrower plot whereas cylinders compact had the lowest peak in the distribution of voronoi cell volumes. On the contrary, the distribution of voronoi cells surface area of spherical particles was with narrower plot and the highest peak due to construction of similar polygonal voronoi cells than for pills and cylinders.

The second study had resulted in more uniform void size distribution for sample of large amount of fine spherical particles in binary mixture. Moreover, the addition of fibers contributed to generation of more packed compacts with small voids. The sample of 1% wt. of fibers, 62%wt. of fine and 37%wt. of coarse spheres demonstrated the smallest median

size of voids $d_{50} = 0.795$ mm and the most uniform voids distribution with sharpness index $d_{10}/d_{90} = 0.345$.

In conclusion, it was found that the non-spherical particles shape can significantly affect to the packing structure of powder compacts. The analyses of void size distribution and Voronoi tessellation can ensure more packed compacts with small-scale voids and smooth voronoi cells construction for irregular shapes of pills and cylinders than spherical particles. Likewise, the inclusion of non-spherical particles contributed to the formation of more packed compacts for ternary mixture of fine and coarse spheres, and fibers.

Acknowledgements

First and foremost, I would like to thank my esteemed supervisors, Prof. Golman and Dr. Yermukhambetova for giving me the opportunity to do research and providing invaluable guidance throughout this research. Their insightful feedback pushed me to sharpen my thesis, and sincerity and motivation have deeply inspired me.

I would like to acknowledge my colleague from research group Zhazira Berkinova for her treasured help in shaping my simulation methods and become friends.

Finally, I would like to express my gratitude to my parents, my siblings, my husband and my mother-in-law for their encouragement and support all through my studies.

Table of contents

Abstract	2
Acknowledgements	4
List of Abbreviations	7
List of Tables	8
List of Figures	9
Chapter 1 – Introduction	10
1.1 General	10
1.2 Aims and objectives	11
1.3 Thesis layout	11
1.4 Contribution	11
Chapter 2 – Literature Review	12
2.1 Packing particles	12
2.2 Numerical analysis and DEM	13
2.3 Superquadrics	15
2.4 Packing structure analysis methods	17
2.5 Voronoi tessellation for packing structure analysis	19
2.6 Conclusion	21
Chapter 3 – Methodology	22
3.1 Particle form generation	22
3.2 DEM simulations	23
3.3 Cross-sectional image analysis preparation	24
3.4 Voronoi tessellation construction	26
3.5 Mixture of fibers with spherical particles	26
3.6 Summary	28
Chapter 4 – Results & Discussion	29
4.1 Shape effect of particles on powder compact microstructure	29
4.2 Effect of non-spherical particles inclusion into spherical powder compact mixture	34
4.3 Summary	37
Chapter 5 – Conclusions and Recommendations	39
Bibliography	41
Appendices	44
Appendix A. Running files sample for PySetVoronoi	44

Appendix B. Colored cross sectional images of pills, cylinders and spheres	46
Appendix C. Colored cross-sectional images of binary mixtures with fibers	49

List of Abbreviations

DEM – Discrete Element Method

VT – Voronoi tessellation

SQ – superquadrics

MS – multispheres

VSD – void size distribution

2D – two-dimensional

3D – three-dimensional

List of Tables

Table 3.1: Visualization of non-spherical particle created using superquadrics.	22
Table 3.2: The mechanical properties of particles and DEM simulation parameters.	23
Table 3.3: Generation parameters of fine and coarse spherical particles, and fibers.	27
Table 3.4: Particle mixture composition for DEM simulations.	27
Table 3.5: The mechanical properties of particles and DEM simulation parameters.	28
Table 4.1: Parameters of void size distributions.	36

List of Figures

Figure 2.1: Simulation of packing spherical particles using DEM [10].	14
Figure 2.2: The continuous parameterization of superquadrics through its five geometrical parameters [19].	16
Figure 2.3: Basic conception of Voronoi diagram [27].	19
Figure 2.4: Application of Voronoi tessellation for spherical (a) and non-spherical (b) mixtures compact [10, 21].	20
Figure 3.1: Visualization of packed compacts using Paraview [33] (a) Domain and region, (b) Simulation 1, (c) Simulation 2, and (d) Simulation 3.	24
Figure 3.2: Cross-sectional images normal to x coordination system for three samples.	25
Figure 4.1: Colored cross-sectional images of three samples normal to x coordination system.	29
Figure 4.2: Normalized cumulative frequency of void size distribution of three samples by (a) x, (b) y, and (c) z directions	30-31
Figure 4.3: Visualization of selected voronoi cells and a single voronoi cell for three samples	32
Figure 4.4: Normalized Voronoi cells volume correlation.	33
Figure 4.5: Normalized Voronoi cells surface area correlation.	34
Figure 4.6: Images of compact cuts from DEM normal to Z direction and respective binary images for Simulation 1 and Simulation 2: a) before, and b) after binarization	35
Figure 4.7: The packed compacts images visualized by Paraview for (a) Simulation 2 and (b) Simulation 4	35
Figure 4.8: Void size distribution for Simulations 1 and 3 measured in (a) X, and (b) Y directions	36
Figure 4.9: Void size distribution for all simulations in z direction.	37

Chapter 1 – Introduction

1.1 General

In the modern world, improving materials properties is a unique request in the chemical and materials engineering in order to provide a better products for human consumption. Particle packing plays an important role in many industrial processes due to its dominant influence on the final product performance [1]. Generally, packing of particles means positioning of particles regarding to the bulk volume without particles overlapping. The complications of packing process can arise from many factors: disorderliness of packing, complexity of networks of particles and pores, and particle parameter effects such as shape and size.

Consequently, special attention should be devoted to the analysis of particle packing in order to develop knowledge that useful for innovations in the materials science and engineering. Many studies considered packing of polydisperse particle mixtures and particles of complex shapes.

The extensive research works [2, 3] have shown that the physical and mechanical characteristics of material are tightly connected to the packing properties. As a consequence, a further thorough understanding the phenomenon of packing particles is of a great significance. It can benefit engineering industries such as powder handling, additive manufacturing for aerospace technology, automotive industry, and advanced engineering applications, soil mechanics, pharmaceutical industry, and other manufacturing of high-value products [4]. The particle packing study is useful both for designing tightly packed materials and also materials with advanced porous structure.

There are still challenging issues in the powder packing investigation related to quantitative description of particle packing and its void space morphology. Many previous research papers have mainly examined the packing of spherical-shaped particles. However, the particle shape can be the key element in the packing of powder compacts. As an example, it was proved that inclusion of fibers improves the final product performance of construction and advanced engineering materials [5, 6]. Therefore, in the recent years, the scientists and engineers are interested in the investigation of non-spherical particles via numerical analysis evaluation of their packing characteristics.

To sum up, there is a need to investigate further of packing characteristics and void space morphology of composite compact of differently shaped particles.

1.2 Aims and objectives

The aim of the study is to analyze packing structure and morphology of powder compacts made of particles of different shapes. In order to achieve it, the research is focused on:

- (1) creation of powder compact with particles of various shapes using the Discrete Element Method,
- (2) analysis of void spaces morphology of powder compact using the Voronoi tessellation and void size distribution methodologies.

1.3 Thesis layout

The thesis organization follows next parts: Chapter 2 is dedicated for literature review of various methodologies of packing of particles compacts and non-spherical form generation using the discrete element method (DEM) and Voronoi tessellation (VT); In Chapter 3, the mentioned methodologies were developed for generation of different packing samples of non-spherical particles compacts and binary mixtures of spherical particles with fibers, and the procedures of the void size distribution and the Voronoi diagram formation; the Chapter 4 considers the results and discussion parts of two studies devoted to estimate packing structure analysis; finally, the conclusions were adopted according to the obtained results and recommendations for future research in Chapter 5

1.4 Contribution

The principal contributions of author are:

- Generation of packed powder compacts of non-spherical particles and binary mixture of spheres with fibers using Aspherix-GUI software.
- Obtaining image analysis of cross-sectional images and construction Voronoi tessellation of the obtained powder compacts on open-source software PySetVoronoi.
- Studying the particle shape effect on the relationship between particles and voids.

Chapter 2 – Literature Review

2.1 Packing particles

The packing of spherical and non-spherical particles is the topical problem in science and engineering which has been approached experimentally and theoretically. The accurate design of particle packing is fundamental for a wide range of applications such as granular materials, composite materials, ceramics, construction materials (sand, rocks, powder, etc.), medicines, glasses, and many other material types [7]. The transport properties of particle compacts such as electrical and thermal conductivities, tortuosity, and compact mechanical properties significantly depend on packing characteristics [8, 9]. Therefore, the research on the packing of spherical and non-spherical particles is of great interest to researchers of advanced materials to create high-quality products.

Majority of early studies have investigated spherical particle compacts due to simplicity of particle shape resulting in easy simulation of particle compaction and quantification of compact structure. The various types of spherical particle packings such as random loose, close and ordered [10] have been studied.

Recently, there has been a growing interest in the study of microstructure and properties of compacts made of irregularly shaped particles. It was noted that the shape of particles significantly influences on the packing characteristics. As an example, Zou and Yu [11] confirmed that the packing density has strong dependency on the shape of particles by varying the aspect ratios of disks and cylindrical particles. Moreover, the oblate spheroids also have represented a positive effect on the packing density rise due to contact numbers growth [12]. Zhao et al. [13] investigated the densification of monosized tetrahedral particles. An important finding was that the deviation of tetrahedral particles shape from the regular tetrahedral form results in the decrease of the frequency of face-face, edge-edge and vertex-face contacts between particles but increase of edge-face contacts.

To sum up, the recent topical question for packing structure investigation is the analysis of compacts of non-spherical shaped particles and it is the subject of interest among many researchers in powder technology and materials science fields. Further studies need to be implemented to give insight into quantitative analysis of compact morphology. Therefore,

this thesis research is aimed at studying the topic of packing powder compacts consisting of irregularly shaped particles.

2.2 Numerical analysis and DEM

The theoretical investigations in engineering have extended gradually in the recent years due to increase in computational power, hence, computer applications have risen interests among many researchers. The computer modeling has shown perspective for many disciplines and, particularly, for the development of computational materials science and engineering. The diversity of numerical analysis can extend the knowledge and understanding of materials properties.

Despite the advances in supercomputers, the simulations are still limited when it comes to complex bodies and assemblies. A few methods can achieve this challenging target. For example, the Discrete Element Method (DEM) developed by Cundall and Strack [14] is used for numerical modeling of bulk powder behavior considering the microscopic interactions between distinct particles.

DEM model equations include equations describing the flow and interaction of particles. The translational and rotational motions of particles are considered and the equations are derived based on the Newton's second law of motion (see Eqs. (1) - (6)).

$$m_i \frac{d^2 x_i}{dt^2} = m_i a_i = F_i, \quad (1)$$

$$v_i = \frac{dx_i}{dt}, \quad (2)$$

$$I_i \frac{d^2 \theta_i}{dt^2} = I_i u_i = T_i, \quad (3)$$

$$w_i = \frac{d\theta_i}{dt}, \quad (4)$$

$$F_i = F_{i,contact} + F_{i,gravity} + F_{i,fluid} + F_{i,external}, \quad (5)$$

$$T_i = T_{i,contact} + T_{i,fluid} + T_{i,external}, \quad (6)$$

where m_i , x_i , a_i , and v_i are the mass, position, acceleration and velocity of particle i , respectively; I_i , θ_i , u_i and w_i the inertia moment, orientation vector, angular acceleration and angular velocity, respectively; T_i and F_i are overall sums of the torques and forces, respectively.

However, Eqs. (1) and (3) are true only for symmetrical particle around its mass center. In the evaluation of a non-spherical particle, the new spatial particle orientation can

affect to the inertia moment regarding time-step change. Regarding the body-fixed coordinate system, the motion eq. (7) is derived to take into account the inertia moment [15]:

$$I_i \frac{dW_i}{dt} + W_i \times (I_i W_i) = \Lambda_i^{-1} T_i, \quad (7)$$

where W_i and T_i the angular velocity of the body-fixed coordinate system and external inertia moment, respectively; I_i and Λ_i^{-1} are the tensor of inertia and transformation matrix to body-fixed coordinate system, respectively.

DEM has been utilized to study diverse phenomena based on the discreteness of complex systems such as powder materials. One of the early research papers has considered using DEM as a powerful tool to investigate particle packing to improve the effectiveness of construction materials [16]. Fig. 2.1 represents the typical process of packing particles. Wu [16] claimed that the implementation of numerical analysis helped to obtain the maximum packing in available volume in the example of reduction of concrete harmful effect on the environment.

However, it is still challenging task for computational research to implement the realistic particle shape to maximize research practicality for manufacturing powder materials. Many conducted studies are based on the DEM codes for particles with ideal spherical shape due to its simplicity and mitigation of large computational expenses associated with simulation of non-spherical particles; on the other hand, it limits the usefulness of such research with ideal spherical shapes for realistic irregular particles.

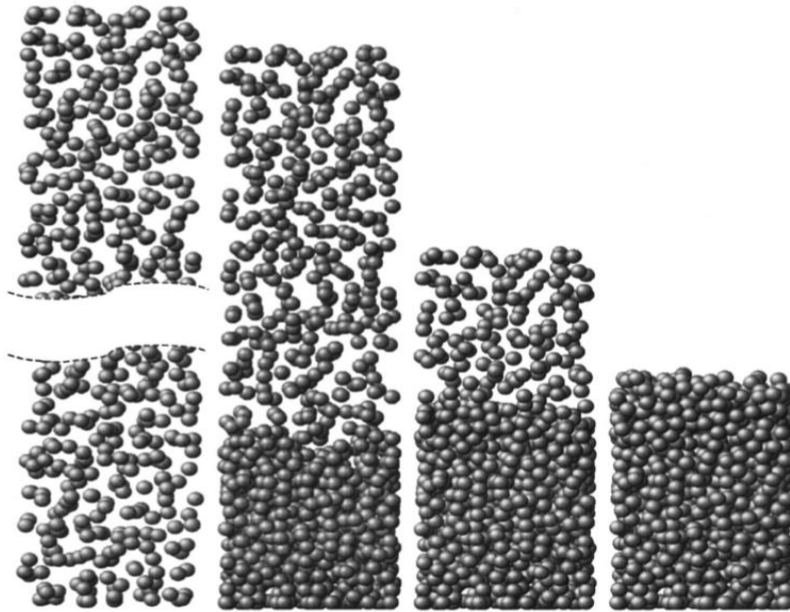


Figure 2.1: Simulation of packing spherical particles using DEM [10].

Recently, the new DEM methodologies such as multispherical (MS) and superquadrics (SQ) have been developed to generate non-spherical shaped particles. [17]. The overlapping spherical particles are used in MS method to generate the particles of desired shape and the SQ method utilizes superquadrics to form particles with sharp or rounded corners. Soltanbeigi et al. [17] applied both MS and SQ methods to show their advanced opportunities for generation of irregularly shaped particles. Consequently, the expectation of better packing for non-spherical shaped particles was proved. In our research, we will apply the SQ method to generate particles of non-spherical shape, as it is simpler and more cost-efficient than the MS method.

Eventually, the literature findings can ensure applicability of DEM to simulate packing process and even generate non-spherical forms of particles via various mathematical approach such as superquadrics and multispheres.

2.3 Superquadrics

The superquadrics have encompassed many computational fields to create various forms and been employed to extend the geometrical properties of particles. One of the applications is the extension of spherical and elliptical shapes to maintain more complex shapes or assemblies of particles. Barr [18] introduced superquadrics in mathematics with the next equation (Eq. (8)):

$$f(x, y, z) = \left(\left| \frac{x}{a} \right|^{n_2} + \left| \frac{y}{b} \right|^{n_2} \right)^{\frac{n_1}{n_2}} + \left| \frac{z}{c} \right|^{n_1} - 1 = 0, \quad (8)$$

where a, b, c are the half length of superquadric in the underlying coordinate axes respectively for x, y, z ; n_1 and n_2 are the blockiness parameters which shows the sharpness of shape. Cylinders, cuboids, ellipsoids, and other forms can be generated using superquadrics approach. The continuous changes in shapes can be achieved through altering five mentioned-above characteristics. Figure 2.2 demonstrates that one can easily generate various superquadric forms by changing the blockiness parameters: blockinesses equal to 2 for ellipsoid construction; if one blockiness is equal to 2 and second one is larger than 2 then eq. (8) constructs cylinders; finally, blockinesses are more than 2 then eq. (8) can construct cuboids [19]. Therefore, these changes of SQ form can smooth the shape and obtain more stable procedures for simulations to define non-spherical shapes.

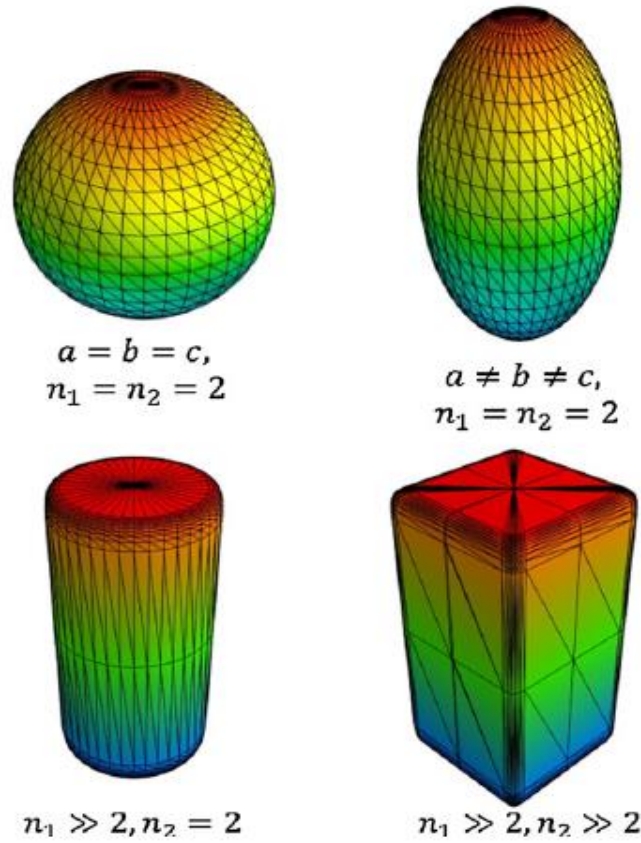


Figure 2.2: The continuous parameterization of superquadrics through its five geometrical parameters [19].

In the last years several packing particles practitioners have become interested in the employment of superquadrics for constructing packed compacts of non-spherically shaped particles. Specifically, most of them examine elliptical shapes in order to compare with spherical particles packings. Gan et al. [20] conducted numerical study based on the DEM simulations for oblate and prolate ellipsoids. Under the effect of vibration in one dimension the increase of the coordination number was obtained for oblates while the prolates have shown reduction due to excluded volume. Moreover, Zhao [21] also pointed out the shape effect of monosized elliptical particles in the triaxial shear testing. Anisotropy of particle orientations due to shape complexity disordered the network of voids during shearing.

Furthermore, Delaney and Cleary [22] demonstrated the profound effect of superellipsoids on packing structure through determination of surface smoothness and irregularity. This work has described the effect of aspect ratio on the rotational degree of freedom. Dong et al. [23] studied the differentiation between SQ forms provided by DEM such as elliptical prolates and oblates, and cylindrical disks and rods. The correlations in

space discretization have been evaluated in three-dimensional case and the findings showed the lognormal distribution for reduced volume and surface area.

Through limited works applying superquadrics, Pereira and Cleary [24] investigated the binary mixture of cuboids as superquadrics and spheres during the segregation process. They noticed the relationship between flow and particle shape as their tendency to place along the tumbler surfaces.

In a summary, it was found that superquadric is applicable for representation of irregular shape for realistic particles of powder materials. The implementation of superquadric shapes regarding its properties and creation of desired forms is amenable for understanding the specific characteristics of non-spherical particles in packing. This thesis work is applied superquadrics to design non-spherical particles and generate corresponding packed compacts.

2.4 Packing structure analysis methods

As aforementioned, the analysis of packing structure is important for understanding and evaluating mechanical and engineering properties of materials. There are many techniques of packing analysis from experiments and simulations to their combinations. The methods can differ in many other aspects related to the investigation of material properties such as by particles characteristics (physical properties, polydispersity, and geometry) and dimensional description (two and three-dimensional analysis).

Combining experimental and numerical analysis is practiced among many researchers. For example, Xia et al. [3] used X-ray tomography and computer-aid research methods to design the structure of packed oblates. The radial distribution function was used to analyze the structural correlation features for orientations of particles and free volume distribution. This work reproduced more experimental validations on their analysis and found that the polydispersity effect influencing packing properties can arise from particle asphericity. In other respects, Wang et al. [25] employed DEM simulations for structural analysis of ceramic breeder pebble beds. This numerical analysis examined deviation of contact numbers and average coordination number due to packing fraction change. However, these types of analysis have limitations regarding several reasons such as only two-dimensional evaluation, less detailed analysis of free space discretization and packing structure features, etc.

One of the popular concepts in the analysis of spatial distribution of objects is the Voronoi tessellation (VT) approach. It refers to technique of partitioning space into the regions close to near points. Scientists initially implemented it for points arrangement, however, its usefulness extended to many different areas from astrology to the marketing [26].

The packing structure researchers have acknowledged the usefulness of VT concept the last decades. Ferrero [27] has underlined the effectiveness of Voronoi tessellation tool to implement numerical analysis of geometrical resolution for crystallography. The idea is to reduce the free space as squared distances on intersections between solid crystals . Moreover, Poupon [28] asserted that packing density of protein molecules can be assessed with VT to determine particle volumes; also, this topological analysis can facilitate the description of system environment either homogeneous or heterogeneous.

Furthermore, this approach has shown a great influence for different space determination as 2D and 3D. For example, the two-dimensional description was obtained to characterize of granular materials structure in planar and corresponding changes of movement [29]. The findings were helpful to study the granular systems stability with rising particles concentration without experiments. However, nowadays many studies are related to three-dimensional consideration of VT to map into natural conditions. Andronov et al. [30] emphasized the VT analysis space partitioning approach to indicate collective properties in a short-range. In addition, the investigations as [21] also depict three-dimensional evaluation of non-spherical particles to obtain thorough void networks analysis and to study the relationship between them.

Finally, it has been known that the various methodologies and tools can analyze packing structure. In literature there are many research papers recognizing the effectiveness of Voronoi tessellation to examine and evaluate structural properties for various areas. This mathematical concept of partitioning space showed its practicality for different conditions like different particle properties (sizes and shapes) and descriptions of dimension. Recent developments in Voronoi tessellation have heightened the need for structural analysis of non-spherical particles packing.

2.5 Voronoi tessellation for packing structure analysis

Originally, Voronoi tessellation was conceptualized to discretize the free space between points. Ferrero [27] demonstrated composing elements of Voronoi tessellation approach such as generator point, vertex and edge. Generator point can be assumed as every point or particles while edges and vertices create line segments. Fig. 2.3 demonstrates simple Voronoi diagram construction and its features.

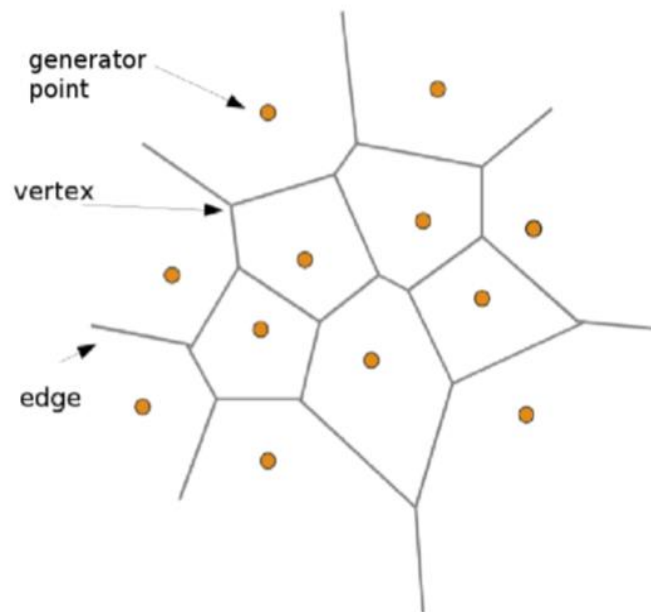


Figure 2.3: Basic conception of Voronoi diagram [27].

Consequently, the VT approach can be estimated as a key element for developing the research area of particles packing analysis. Yi et al. [10] studied the packing of ternary mixture of spherical particles containing large, median and small sizes of spheres. However, the work is limited to particles of spherical shape. Zhao et al. [21] considers monodisperse elliptical particles mixture and employs three-dimensional Voronoi analysis to compare the asphericity effect by simulations in DEM. The VT estimations provided the properties such as local porosity and reduced surface area constituted by void and particle networks relationship. The interesting finding was the tendency of Voronoi cells surfaces softening which was greatly affected by particle shape effect.

The differences regarding to particle shape effect between Voronoi cells generation for multiradial-spherical and monodisperse elliptical particles are represented in Fig. 2.4 [10, 21].

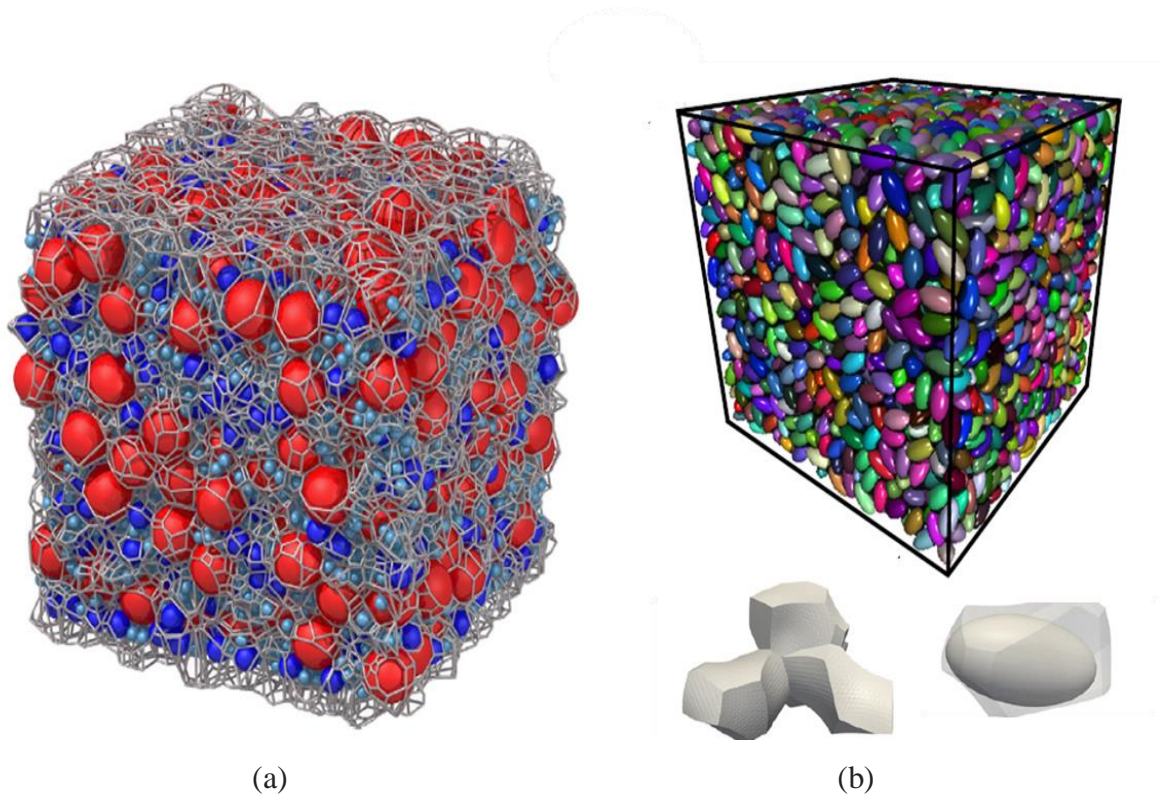


Figure 2.4: Application of Voronoi tessellation for spherical (a) and non-spherical (b) mixtures compact [10, 21].

Similarly, Luchnikov et al. [31] studied the fiber network using Voronoi diagram, and Dong et al. [23] investigated the packings of ellipses and cylinders using the radical VT. To the best of our knowledge, the detailed analysis of packing structures of non-spherical particles is still challenging to the complex shapes of particles.

To sum up, the Voronoi tessellation might be suggested as one of the most applicable tool to characterize the topological organization of complex networks. The Voronoi diagram can dominate among other analysis methods due to detailed determination of spatial geometry for many engineering practices. It covers multitude features of packing powder compacts such as polydispersity, mixtures, particle shape adoption and others. As a result, the adoption of this concept can benefit thesis topic study and develop its methodology.

2.6 Conclusion

In conclusion, packing of powder compacts plays a key role for materials science and engineering to create and manufacture high-quality products. It is known that the discrete element method is one of the most applicable method to compute the constructions of packed compacts with distinct particles. Moreover, it can cover different aspects for generation of complex particle shapes to closely introduce them into realistic conditions. The superquadrics have been introduced as a powerful tool to represent irregular shape and comparatively easy application to generate its form.

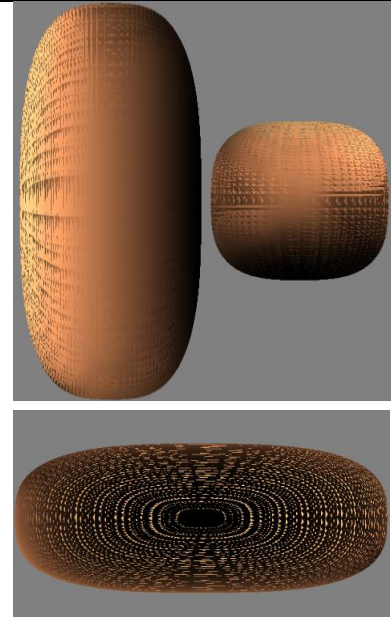
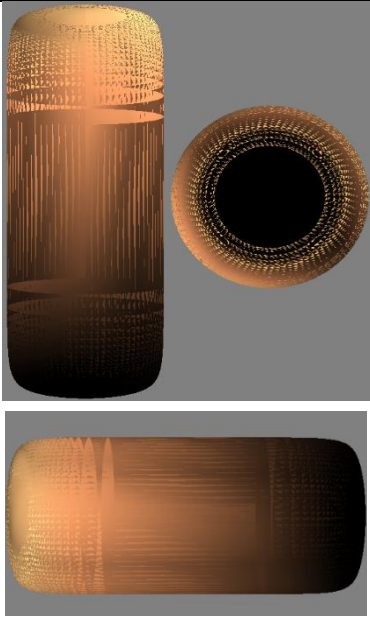
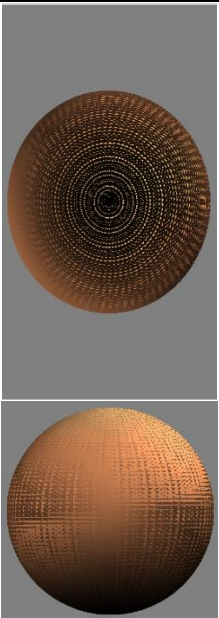
Therefore, the present research aims at providing more detailed analysis of non-spherical shaped particulates and their effect on the packing of powder compacts. Furthermore, application of Voronoi tessellation to the characterization of compact microstructure can significantly extend study of powder materials.

Chapter 3 – Methodology

3.1 Particle form generation

The particles of the desired non-spherical shape were generated by varying the superquadric parameters. The particle shape and size depend directly on superquadric geometrical parameters such as half lengths along x, y, and z coordinates and sharpness index (blockiness in DEM simulations). The particles generated using superquadric approach are shown in Table 3.1 together with corresponding superquadric parameters.

Table 3.1: Visualization of non-spherical particle created using superquadrics.

			
	<i>Pill</i>	<i>Cylinder</i>	<i>Sphere</i>
a , m	0.004	0.004	0.0061
b , m	0.004	0.004	0.0061
c , m	0.01	0.0095	0.0061
n_1	3	10	2
n_2	3	2	2

The simulation of packing compacts has employed these forms of superquadrics and, thus, there are three possible powder compacts in the evaluation. In order to compare thoroughly the effect of shape differences, the superquadric parameters were adjusted in such a way that superquadrics have similar volumes.

3.2 DEM simulations

This study considers three powder compacts of non-spherical particles in the consideration of superquadric shape differences. The samples were simulated using Aspherix-GUI software package [32] based on the DEM. The Table 3.2 summarized the DEM simulation setting parameters.

Three samples have equal domain size $0.4\text{m} \times 0.4\text{m} \times 0.6\text{m}$ and number of particles 45,000. The domain, region of superquadric particles formation and orientation of simulated boxes are illustrated in Fig. 3.1(a). The flow of particles with random orientations has closely resembled the flow of realistic powder particles in Z direction under gravity. The Simulation 1 is with pills shaped superquadrics particles illustrated in Fig. 3.1 (b), the Simulation 2 with cylinders in Fig. 3.1 (c) and the Simulation 3 with spheres in Fig. 3.1 (d).

Table 3.2: The mechanical properties of particles and DEM simulation parameters.

Mechanical properties	Young's modulus, [Pa]	5×10^6
	Poisson ratio	0.4
	Restitution coefficient	0.6
	Friction coefficient	0.4
DEM parameters	Time-step, Δt [s]	1×10^{-5}
	Gravity, g [m/s^2]	9.81
Particles physical properties	Density, kg/cm^3	2500

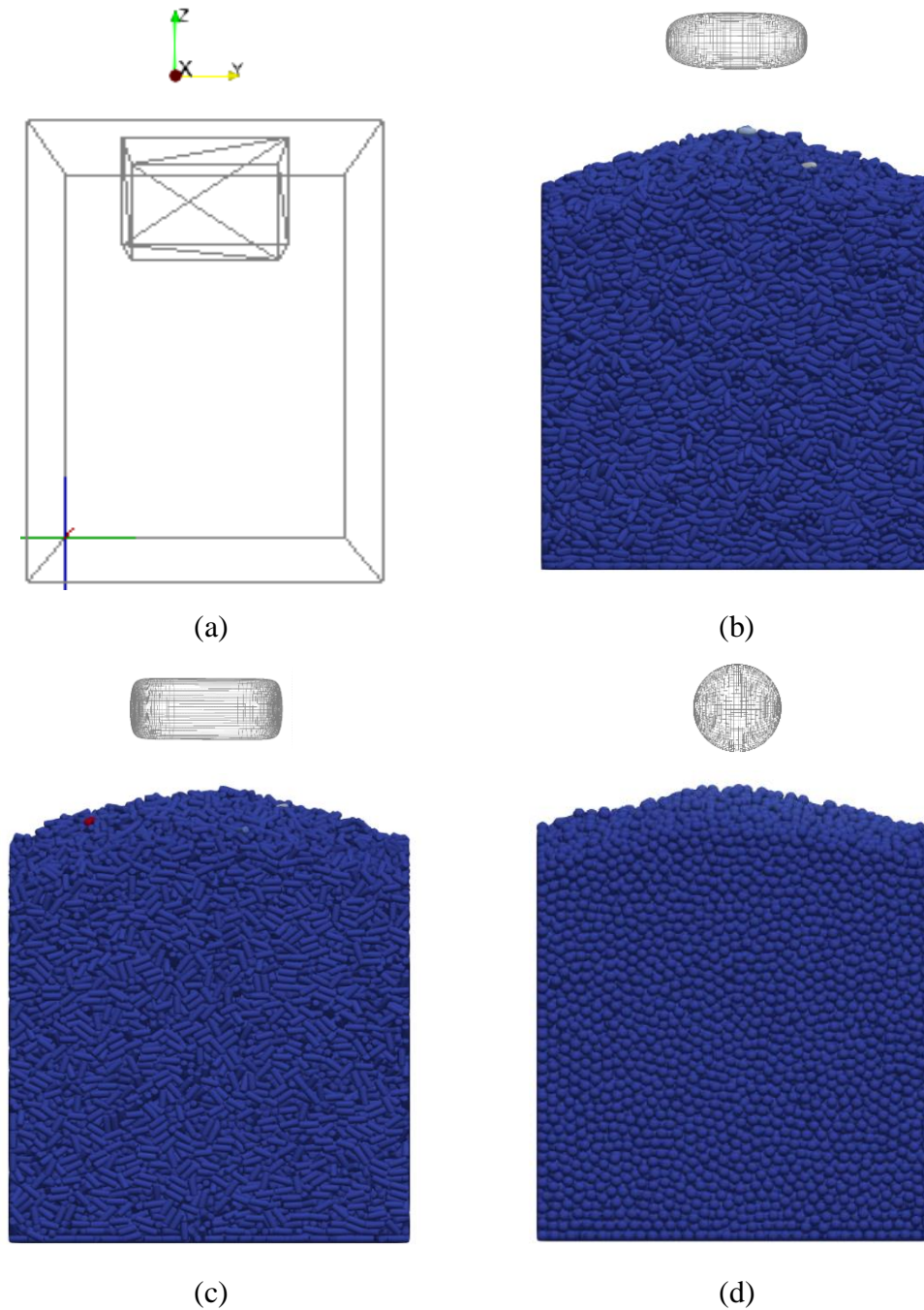


Figure 3.1: Visualization of packed compacts using Paraview [33] (a) Domain and region, (b) Simulation 1, (c) Simulation 2, and (d) Simulation 3.

3.3 Cross-sectional image analysis preparation

The analysis of packing structure for non-spherical particles compacts was based on the cross-sectional ImageJ Analysis [34] methodology. Three specimens of non-spherical particles compacts were visualized in Paraview and respective cross-sectional images

normal to x, y, and z coordinate systems were extracted for further packing analysis. In order to eliminate wall-particle effect, images of cross-sections were cut by each side. Figure 3.2 shows prepared images for pills, cylinder, and spherical particles compacts in x direction.

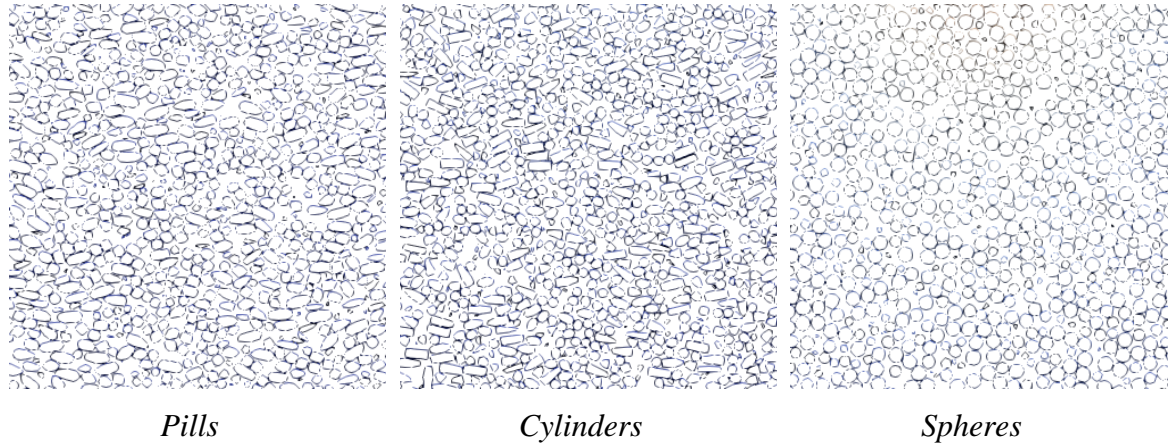


Figure 3.2: Cross-sectional images normal to x coordination system for three samples.

The concept of void size distribution (VSD) was used to explain quantitatively the packing structure of three different samples related to their particle forms. The algorithm developed to estimate VSD has several steps to evaluate the void characteristics:

1. As shown in the figures above three-dimensional images of compacts visualized by Paraview software were employed to obtain cross-sectional images normal to x, y, and z directions;
2. ImageJ Analysis open-source software utilized taken images from DEM to create the required binary images for further quantitative analysis. The colored images were edited to clearly separate particles and voids in order to prepare for the next step of VSD Macro analysis.
3. The final step was to measure void sizes on two-dimensional cross-sectional images by randomly placing the circles of voids of various sizes. The each trial is assumed to be successful if the circle do not touch or overlap particles. The total number of trials was 15,000 for each void size based on preliminary results. Then, the probability of successfully locating circles in the void spaces was calculated as the ratio of successful trials to the total number of trials and the void size distribution was plotted as the probability versus void circle size.

3.4 Voronoi tessellation construction

The Voronoi tessellation analysis uses output information from DEM simulations such as center coordinates of particles, half lengths along the x , y , and z coordinates, sharpness index as blockiness and rotation matrix as quaternions.

The orientation of non-spherical particles was expressed by rotation matrix. The mapping from local to global coordinate systems is featured through rotation of coordinate vectors $\{e_1, e_2, e_3\}$ and the rotation vectors or quaternions can track these changes of the space orientation [35].

The quaternion of rotation q is calculated from the rotation angle α and the related unit axis e :

$$q = (q_0, q_1, q_2, q_3)^T = \cos(\alpha/2) + e \sin(\alpha/2), \quad (8)$$

There are four elements of rotation matrix such as $quat_0$, $quat_1$, $quat_2$, and $quat_3$ expressed in the following equations (9-10):

$$A = \begin{pmatrix} 1 - 2(q_2^2 + q_3^2) & 2(q_1q_2 - q_0q_3) & 2(q_1q_3 + q_0q_2) \\ 2(q_1q_2 + q_0q_3) & 1 - 2(q_1^2 + q_3^2) & 2(q_2q_3 - q_0q_1) \\ 2(q_1q_3 + q_0q_2) & 2(q_2q_3 + q_0q_1) & 1 - 2(q_1^2 + q_2^2) \end{pmatrix}, \quad (9)$$

$$A \cdot e_1 = \hat{e}_1, \quad A \cdot e_2 = \hat{e}_2, \quad A \cdot e_3 = \hat{e}_3, \quad A^{-1} = A^T \quad (10)$$

The open-source Pomelo (PySetVoronoi) software [21] was used to construct the Voronoi diagram and to calculate its features. Three files are required to run the program: input file (particle parameters), test.py (running file), and wall.data (domain size parameters). The samples of program files can be found in Appendix A.

3.5 Mixture of fibers with spherical particles

This part of simulations was focused on the effect of non-spherical particles inclusion into spherical particles mixture. The DEM methodology was used to simulate various mixtures of non-spherical and spherical particles created by using the superquadrics approach. Table 3.3 depicts the visualization of particle forms generation such as coarse and fine spherical particles and elongated elliptical particles. Four specimens of powder

compacts engaged different particles fractions that consist of spherical particles and fibers (Table 3.4). In particular, the inclusion of fibers was carried out for 1% weight-based case and the different fraction between fine and coarse spherical particles represented in Table 3.4.

The same algorithm of Void Size Distribution concept was applied for these four specimens. There was the identical way of processing cross-sectional images to estimate void sizes using Macro tool in ImageJ Analysis. However, the trial numbers were twice increased to 30,000 times for each void circle size.

Table 3.3: Generation parameters of fine and coarse spherical particles, and fibers.


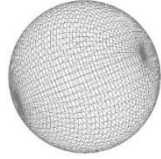

	 <i>Fine spherical</i>	 <i>Coarse spherical</i>	 <i>Fibers</i>
a , m	0.002	0.004	0.0002875
b , m	0.002	0.004	0.0002875
c , m	0.002	0.004	0.006
n_1	2	2	2
n_2	2	2	2

Table 3.4: Particle mixture composition for DEM simulations.

\wt. %	Fine	Coarse	Fiber
Simulation 1	63	37	0
Simulation 2	62	37	1
Simulation 3	40	60	0
Simulation 4	40	59	1

In order to increase time and cost efficiency of simulations, the particle shape and size parameters were changed. The fiber size has been increased to achieve the reasonably large time step (4×10^{-6} s) for DEM simulations setup.

The mechanical properties of each particle in this part of investigation refer to Soltanbeigi et al. [17], and density characteristics are from [36] and [37] (Table 3.5).

Table 3.5. The mechanical properties of particles and DEM simulation parameters.

Mechanical properties	Young's modulus, [Pa]	10^7
	Poisson ratio	0.3
	Restitution coefficient	0.6
	Friction coefficient	0.3
DEM parameters	Time-step, Δt [s]	$4 \cdot 10^{-6}$
	Gravity, g [m/s^2]	9.81
Particles physical properties	Density, kg/cm^3	2500 (spherical particles) 1140 (fibers)

3.6 Summary

To sum up, the simulations were conducted in two ways: investigation of shape differences of monodisperse particles compacts and study of the effect of non-spherical particles inclusion into spherical particles compact on the effect of the packing structure change.

First, DEM simulations and superquadrics approach were employed to generate three different forms of particles and their respective particle compacts. The cross-sectional images of each samples were analyzed by void size distribution method to estimate the voidage with elimination of wall-particle effect. Additionally, the VT analysis was implemented to construct Voronoi diagram using DEM output parameters of particles in their mechanical stable position.

Second, the binary mixtures of spherical particles with the inclusion fiber-like particles ($f_{fine}:f_{coarse}:f_{fiber}$ 63:37:0, 62:37:1, 40:60:0, and 40:59:1) were simulated by DEM. The research method follows DEM simulations in the initial step and, then, implementation of image analysis of cross-sectional cuts to study the void size distribution. There reflected the results of void size distribution for variously fractioned powder compact samples.

Chapter 4 – Results & Discussion

The study of the particle shape effect on powder compact microstructure includes quantitative analyses of two types. The quantitative analysis based on the void size distribution considers two-dimensional cross-sectional images of three different specimens while Voronoi tessellation analysis estimates the three-dimensional arrangement of particles and voids of these specimens.

4.1 Shape effect of particles on powder compact microstructure

Void size distribution. The study initially considered the void size distribution among the void space between particles. Figures 4.1 illustrate the void size distributions of pills, cylindrical, and spherical particle compacts in the cross-sections normal to the x-axis. The visual observation of images confirms that compacts of non-spherical particles such as pills and cylinders show smaller voids with more narrow size distribution than compacts of spherical particles. The cross-sectional images normal to the y and z-axes are summarized in Appendix B.

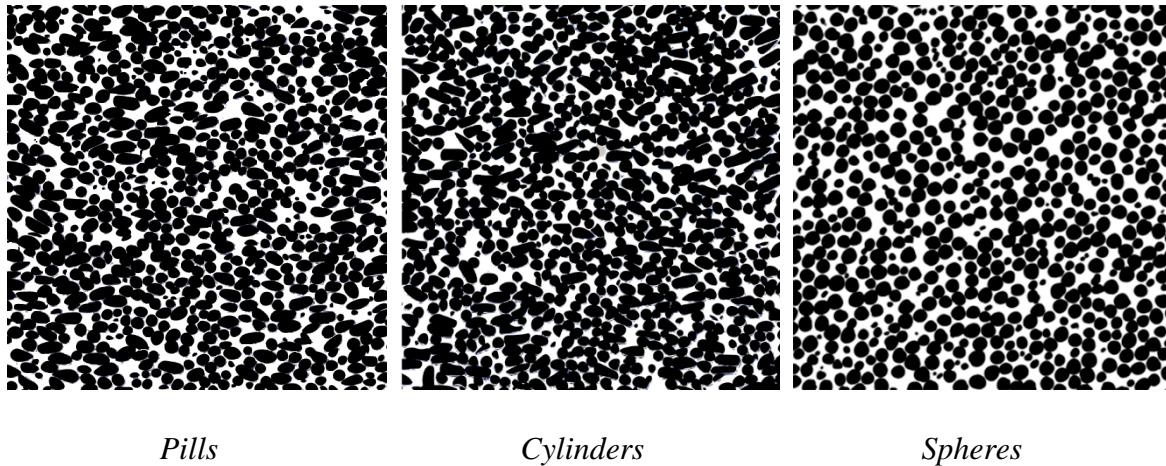
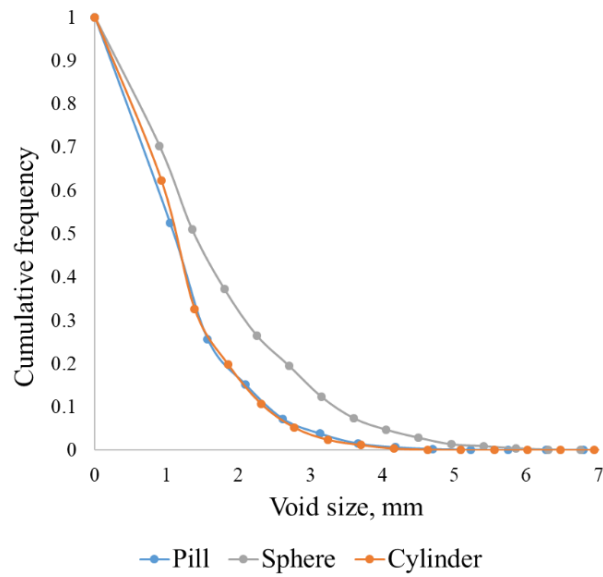


Figure 4.1: *Colored cross-sectional images of three samples normal to x coordination system.*

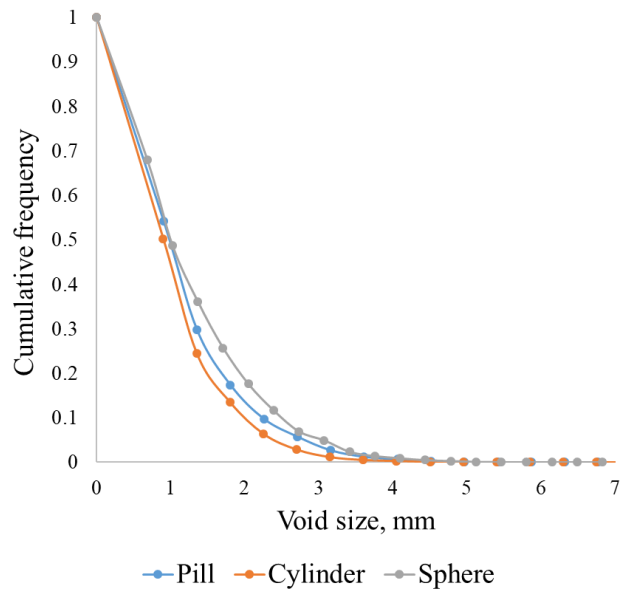
Fig. 4.2 represents cumulative frequency of void size distribution through three samples constructed from superquadric particles as pills, cylinders, and spheres through x, y, and z coordinates. The Fig. 4.2 (a) and (b) demonstrates clear differences between voids

in compacts of idealized shape of spheres and non-spherical pills and cylinders compacts. The irregular form of pills particles and cylinders affected to the less percentage of wide voids among x and y directions.

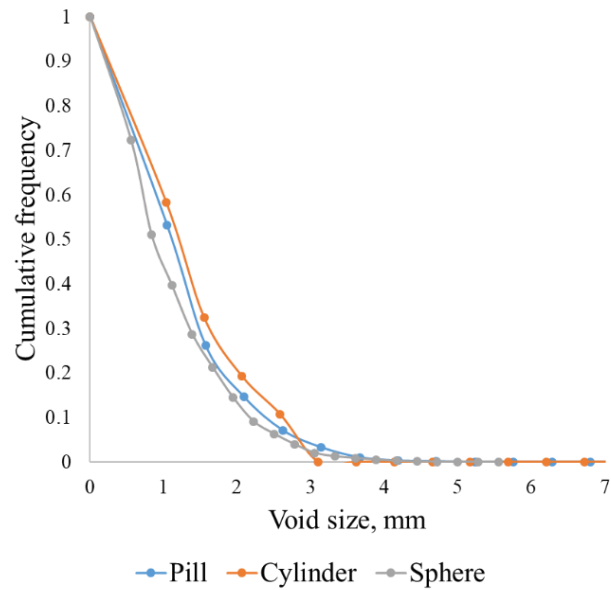
However, due to the flow of particles conducted in z direction the non-spherical particles showed orientation anisotropy. As a result, it affected to the formation of larger voids for pills and cylinders samples whereas spheres samples generated smaller voids in z direction consideration in Fig. 4.2 (c).



a)



b)



c)

Figure 4.2: Normalized cumulative frequency of void size distribution of three samples by (a) x, (b) y, and (c) z directions.

Voronoi tessellation analysis. This part of study relates to the three dimensional characterization of compacts using Voronoi tessellation concept. In order to eliminate wall effect all three samples were processed to cut out for 25% from overall non-spherical particles compacts. Consequently, each compact had about 20,000 particles that were exercised to construct Voronoi diagram.

The visualization of voronoi cells for each superquadric sample is in Figure 4.3. Only five voronoi cells are selected for pills, cylinders, and spheres samples to show how free space has been separated in each case of different shape of particles. Moreover, a voronoi cell is shown for a single pill, cylinder, and sphere particles. The difference in the voronoi cell is connected with the shapes of particles themselves: for spherical it is like a polyhedron whereas for pill and cylinder it is more elongated irregular form cell.

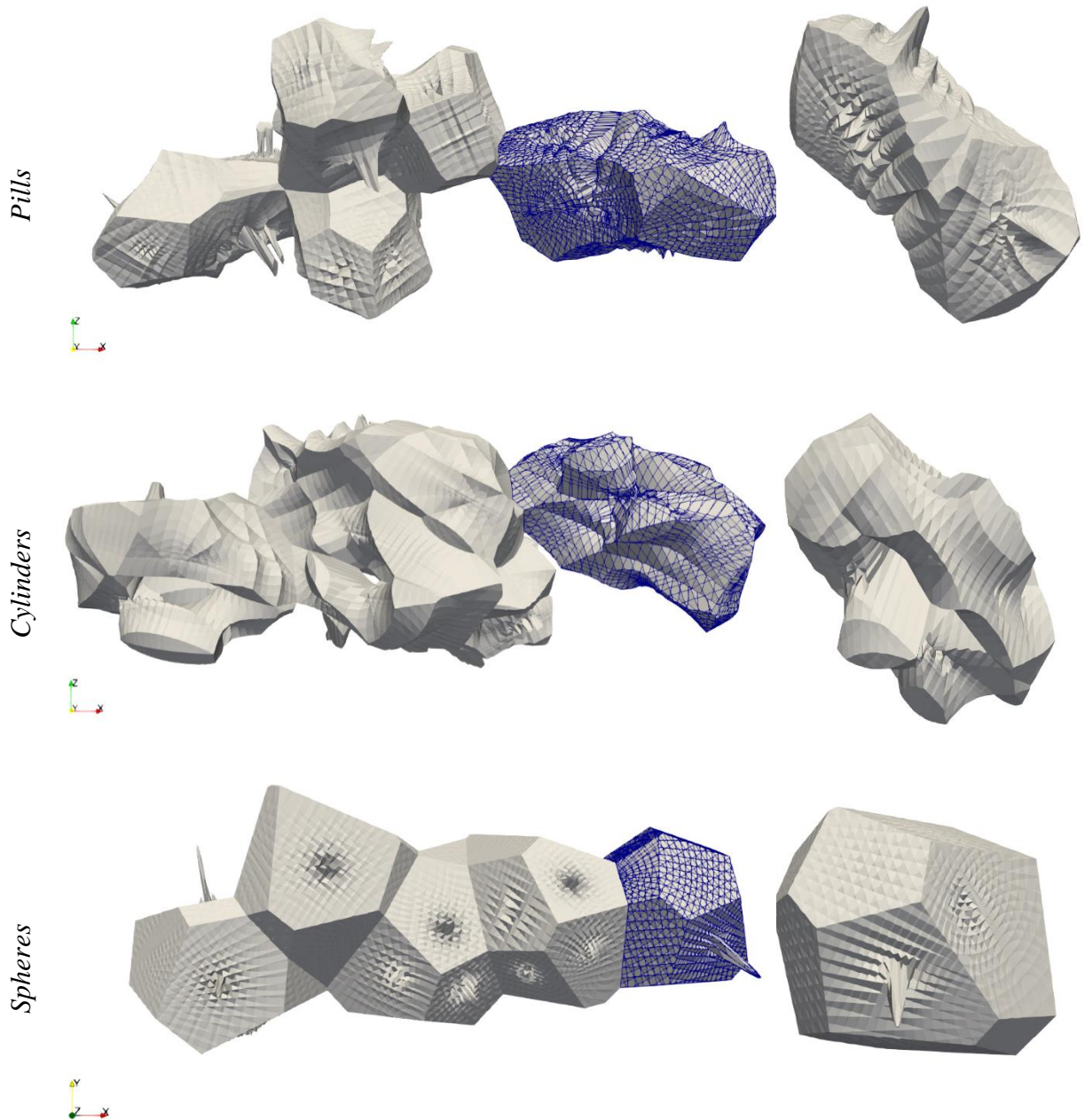


Figure 4.3: Visualization of selected voronoi cells and a single voronoi cell for three samples.

The Voronoi tessellation analysis is based on the characterization of voronoi cells. Figures 4.4 and 4.5 relate to the volume analysis and surface area analysis of voronoi cells. The initially constructed histograms were normalized for all samples outputs to provide more uniform charts with similar area. This method shows accurate difference between charts.

According to Fig. 4.4, the distribution of voronoi cell volume of cylindrical particles compacts illustrated wider plot than pills and spherical particles compacts features. The plot

of cylindrical non-spherical particles covers larger range of cell volume scale. However, the pills particles presented the highest peak of voronoi cell volume than other two samples. It seems to be more uniform distribution of voronoi cells and similar volume for pills formed particles samples.

The distributions in Fig 4.5 examine cells surface areas correlation to compare voronoi cells of three superquadric samples. The same manner of normalization was employed in the construction of these distributions to adjust accurately similar areas under plots. As in cell volumes correlation, cylindrical particles produced wider range of voronoi cells surface area with less range of their distribution. In comparison, the spheres demonstrated the production of less numbers of cells surface area in observing the highest peak and dominance in left-hand orientation of its plot.

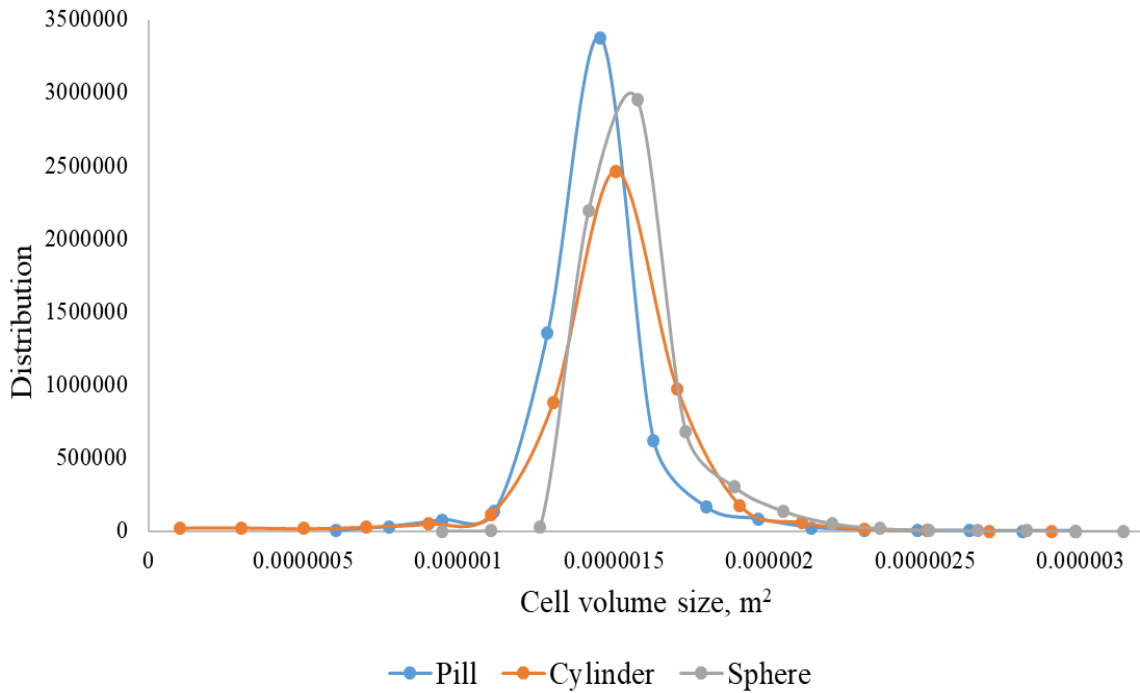


Figure 4.4: Normalized Voronoi cells volume correlation.

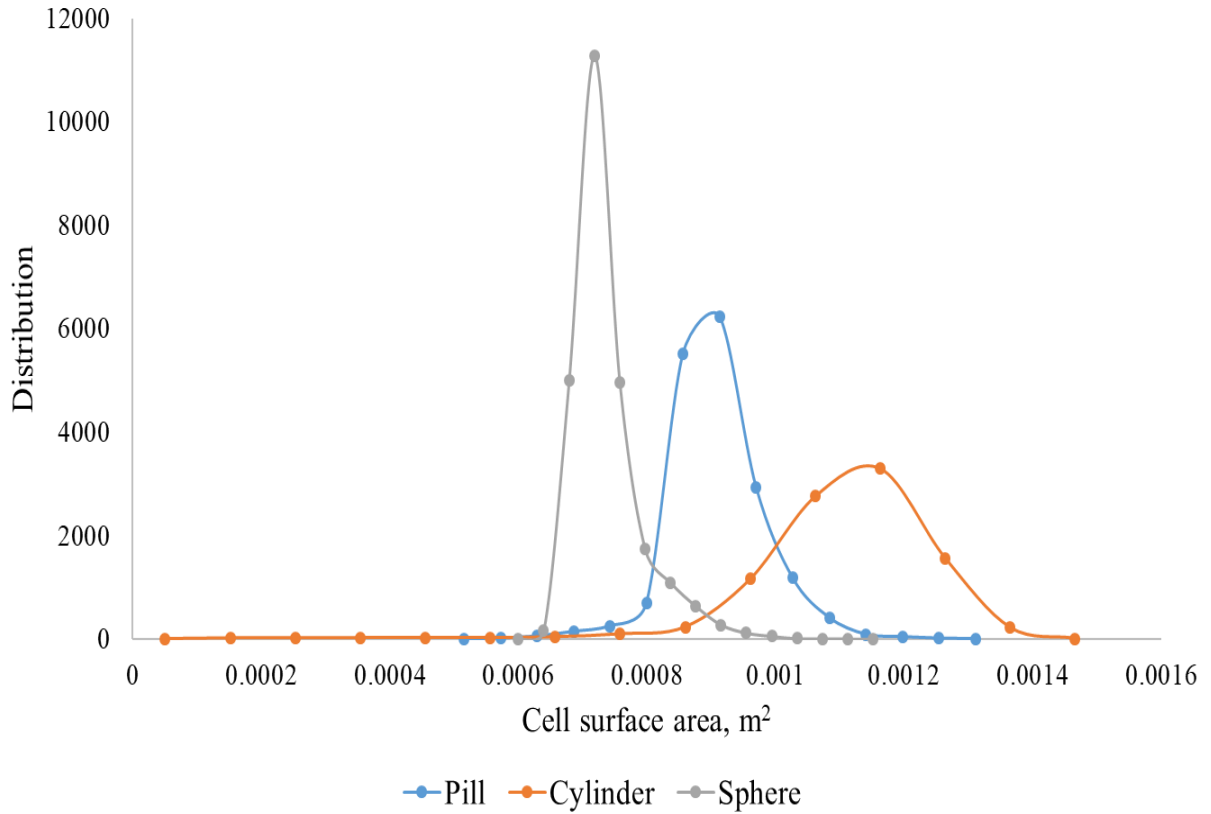


Figure 4.5: Normalized Voronoi cells surface area correlation.

4.2 Effect of non-spherical particles inclusion into spherical powder compact mixture.

The study of the non-spherical particles inclusion into spherical particles mixture has employed the quantitative analysis of void size distribution. The various cases of fiber inclusion were examined into binary compacts of spherical particles. Figure 4.6 shows the processing of cross-sectional images obtained from Paraview and the differences between only spherical particles compact and inclusion of fibers into the same compact. The orientation of fibers as non-spherical elongated elliptical particle is dominated along x and y directions (Fig.4.7). The fibers show anisotropic characteristic due to DEM simulation settings, particularly, the flow of particles was setup along z direction (Fig. 4.7).

Other figures of cross-sectional images are in the Appendix C.

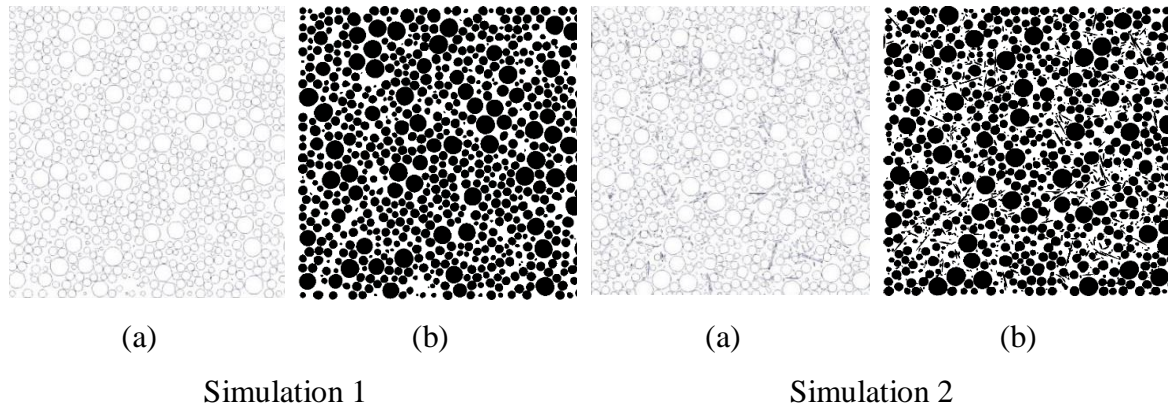


Figure 4.6: Images of compact cuts from DEM normal to Z direction and respective binary images for Simulation 1 and Simulation 2: a) before, and b) after binarization.

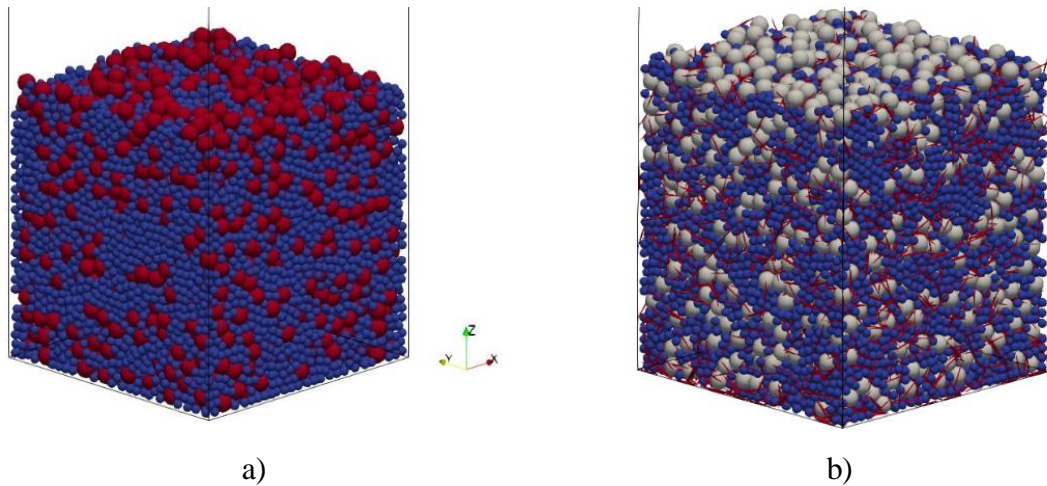


Figure 4.7: The packed compacts images visualized by Paraview for (a) Simulation 2 and (b) Simulation 4.

The cumulative frequency of VSD for compacts of binary mixtures consisting of only fine and coarse spherical particles are presented in Figure 4.8 for x and y directions. The related void features such as median size and sharpness indices are shown in Table 4.1. The size ratio between fine and coarse particles were 1:2 in a radius and only particles fraction changed. For example, the fine spherical particles fraction was adjusted from 63% (major part of compact) and 40% (less part of compact).

The similar trends for all powder compacts were observed in x, y, and z directions. A large fraction of fine particles in the binary mixtures packing affected to the increase of the packing density, the decrease of voids sizes and uniform distribution of voids. Such changes have been detected for fraction of 63%wt. of fine and 37%wt. coarse particles mixture. The indices of median void size had shown decrease from 1.068 mm in Simulation

1 and 0.914 mm in Simulation 3. In addition, the index of sharpness also differs from 0.311 to 0.339 in the case of fine particles amount increase in the same Simulations 1 and 3. It indicates narrower void size distribution and conforming small voids. These tendencies are expressed for x and y directions orientations of packed compacts.

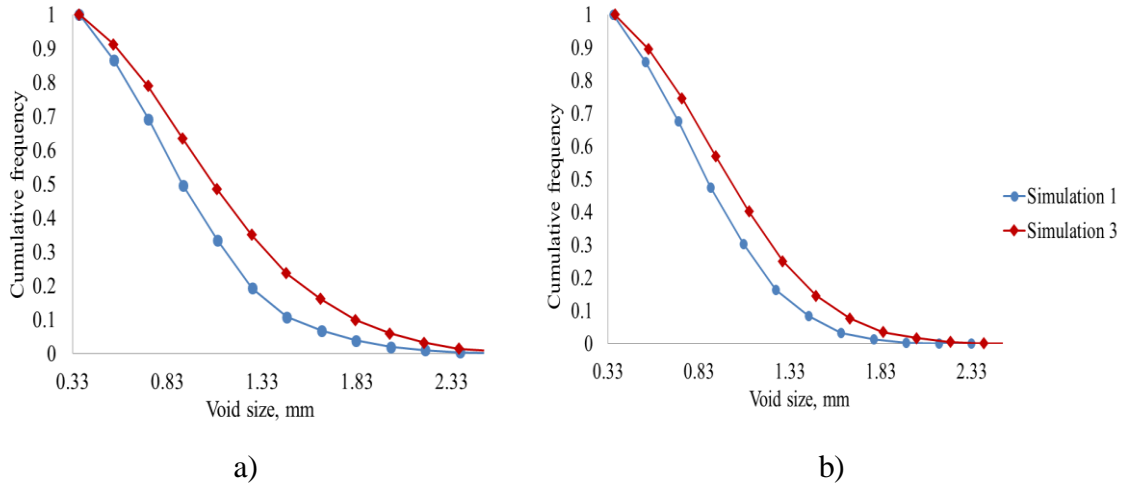


Figure 4.8: Void size distribution for Simulations 1 and 3 measured in (a) X, and (b) Y directions.

Table 4.1: Parameters of void size distributions.

Parameters		d_{50}	d_{90}	d_{10}	d_{90}/d_{10}
Simulation 1 (63:37:1)	x	0.914	0.500	1.475	2.950
	y	0.864	0.490	1.390	2.837
	z	0.930	0.485	1.626	3.353
Simulation 2 (62:37:1)	x	0.940	0.528	1.530	3.211
	y	0.900	0.500	1.457	2.944
	z	0.795	0.437	1.268	3.109
Simulation 3 (40:60)	x	1.068	0.570	1.830	2.898
	y	0.998	0.540	1.590	2.914
	z	0.984	0.533	1.657	2.949
Simulation 4 (40:59:1)	x	0.960	0.540	1.550	2.870
	y	0.965	0.540	1.515	2.806
	z	0.870	0.475	1.380	2.905

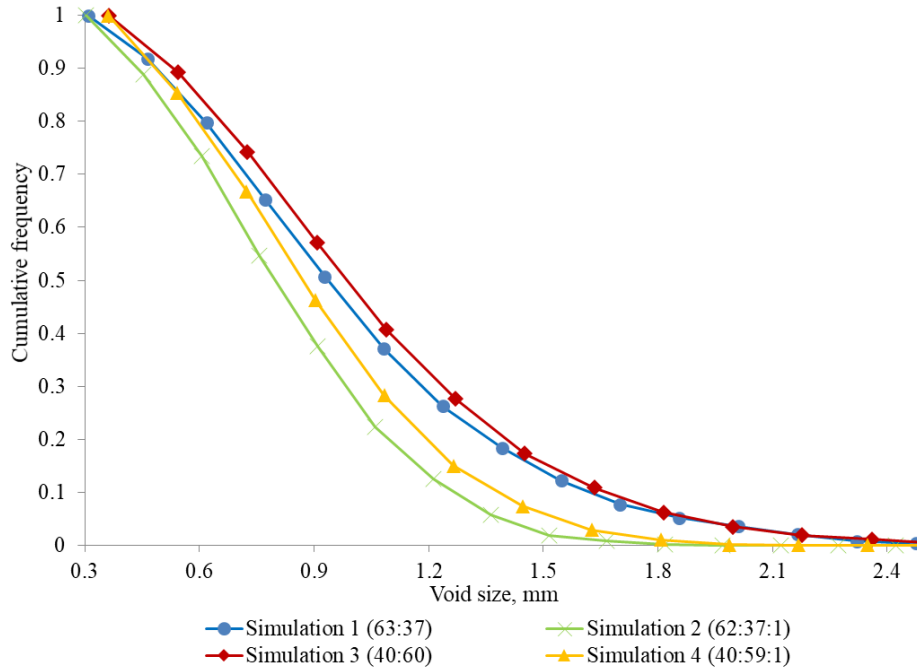


Figure 4.9: Void size distribution for all simulations in z direction.

In case of fibers inclusion, the ternary mixtures consisting of two types of spheres and fibers (1 wt.%) were examined. The addition of fibers had an expected impact on the microstructural character of compacts. The void size distributions were differed significantly due to the elongated non-spherical form of fiber particles and preferences in their orientation in z direction (see Fig. 4.9). The inclusion of fibers for both binary mixtures of spheres demonstrated the decrease of void sizes and sharper void size distributions. Eventually, the densest packed compact was obtained for ternary mixture with $f_{fine}:f_{coarse}:f_{fiber}$ 63:37:1, the smallest voids $d_{50} = 0.795$ mm and the most uniform distribution of voids $d_{10}/d_{90} = 0.345$.

4.3 Summary

In a summary, the two types of studies were carried out in order to investigate the packing structure change of powder compacts according to non-spherical shapes of particles. The first type of studies attempted to characterize quantitatively the packing structure of differently shaped particle compacts and the second one to the packing structure of compacts of spherical particle mixture with inclusion of fibers.

Firstly, three packed compacts under gravity were differed in the particles form such as pills, cylinders, and spheres. The research work was target-related to compare non-spherical form with spherical form of particle. The two quantitative analyses were used to

three samples of compacts to thoroughly investigate the relationship between particles and voids.

The two-dimensional analysis of cross-sectional images normal to x, y, and z directions of three compacts was conducted to measure the void size distribution. The binary images have been examined for voids characterization. As a result, the more uniform distribution of void and small sizes of voids were obtained for pills and cylinders compacts in x and y directions, on the contrary, the symmetrical shape of spheres led to wider voids distribution. Moreover, the Voronoi tessellation concept was also used to quantitatively analyse the voids network in three-dimensional case. The demonstrative feature was Voronoi diagram and voronoi cells generation. It was found that the distributions of voronoi cell volumes of non-spherical particle compact uniformly distributed with high peaks whereas the spherical particles compact had shown the uniform distribution with lower surface area of voronoi cells. The cylinders compact demonstrated wider range of voronoi cells volume and surface area due to its shape sharpness. As a result, the effect of particles shape from ideal spherical to irregular forms can significantly impact to the free space distribution between particles and packing density of compact.

Secondly, four specimens were simulated under the same conditions with the difference in weight-based fractions of fine and coarse spheres, and fibers. The analysis of void size distribution was employed. The finding was more uniform distribution of voids according to sharpness index and the smallest median size of voids for binary mixture of large amount of fine particles. However, inclusion of fibers into binary mixtures has shown more uniform void size distribution and the smallest voids. Eventually, the addition of non-spherical particles in the form of elongated elliptical fibers into spherical mixtures developed more packed compacts in contrast of compacts of spherical particles.

Finally, the non-spherical shaped particles compacts and fiber inclusion into spherical particles mixture were studied. In both cases it was proved that irregular shape of particles can have important influence on the packing structure of powder compacts.

Chapter 5 – Conclusions and Recommendations

In conclusion, the thesis work consists of literature review, methodology, results and discussion parts dedicated to the analysis of packing structure of powder compacts. The literature review considers various methods used for estimation of packing microstructure of compacts. Therefore, from literature the DEM was implied as the modeling method of the simulation of packed compacts. The analysis of packing structure applied image analysis and Voronoi tessellation methods. The settings of simulations were regulated due to the concerns of cost and time efficiency regarding chosen methodologies.

The research works covered different simulation parts such as the first part of differently shaped particles compacts comparison and the second part of effect of inclusion non-spherical particles into spherical particles compact.

The first study applies DEM simulation for generation of three samples with different shapes such as pills, cylinders, and spheres for 45,000 particles in the fixed domain. Then, the image analysis of cross-sectional images provides evaluation of void size distribution for each compact in all x, y, and z directions. Additional voids characterization analysis is obtained with construction of Voronoi diagram for three-dimensional separation of free space between particles for each sample.

The second study also makes use of DEM in order to simulate four specimens containing three types of particles such as fine and coarse spherical, and fibers $f_{fine}:f_{coarse}:f_{fiber}$ 63:37:0, 62:37:1, 40:60:0, and 40:59:1. The similar methodology of image analysis is applied for cross-sectional images normal to x, y, and z directions of each specimen to measure the void size distribution.

Study on the effect of differently shaped particles compacts

Three samples of pills, cylinders, and spheres compacts showed the tendency of non-spherical form influence on the packing structure. Firstly, the more uniform voids size distribution with small voids are obtained for samples of pills and cylinders in x and y directions. However, the anisotropy of non-spherical shape of particles affected to the wider range of voids with larger sizes in comparison with spheres in z direction. Secondly, the Voronoi tessellation constructed more smooth voronoi cells for pills and cylinders. The distributions of volume and surface area of voronoi cells showed narrower plot with high

peak for pills compact while cylinders due to sharpness of particle shape represented wider range of voronoi cell volumes and surface area. The spherical particles compacts represented the shorter plot with wider range of voronoi volume cells and the highest peak with less range of voronoi cell surface area.

Study on the effect of fiber inclusion into spherical particles mixture

The simulated four specimens with and without inclusion of fibers demonstrated significant contrast in the evaluation of void size distribution. The specimen with large amount of fine particles and 1% wt. fibers addition $f_{fine}:f_{coarse}:f_{fiber}$ 63:37:1 indicated the smallest voids with median size $d_{50} = 0.795$ mm and the most uniform voids distribution with sharpness index $d_{10}/d_{90} = 0.345$.

Future Recommendations

The further research needs to be provided for evaluation of other superquadric forms. The Voronoi tessellation can be extended to analyze packing microstructure of complex bodies of superquadric compacts and mixtures of non-spherical particles. For example, there needs in the development of methodology for consideration of binary mixture of spherical particles with inclusion of fibers. Furthermore, different aspect ratios and sharpness of superquadric shapes formation can also be implemented in order to analyze in two-dimensional and three-dimensional analyses of particles and voids networks. Additionally, despite still limited numbers of algorithms based on Voronoi tessellation the new algorithms can be compared to observe more time and cost efficient option.

Bibliography

1. Dullien, F. A. (2012). Porous media: fluid transport and pore structure. Academic press.
2. Athanassiadis, A. G., Miskin, M. Z., Kaplan, P., Rodenberg, N., Lee, S. H., Merritt, J., ... & Jaeger, H. M. (2014). Particle shape effects on the stress response of granular packings. *Soft Matter*, 10(1), 48-59.
3. Xia, C., Zhu, K., Cao, Y., Sun, H., Kou, B., & Wang, Y. (2014). X-ray tomography study of the random packing structure of ellipsoids. *Soft Matter*, 10(7), 990-996.
4. Liu, D. M., & Lin, J. T. (1999). Influence of ceramic powders of different characteristics on particle packing structure and sintering behaviour. *Journal of materials science*, 34(8), 1959-1972.
5. SUBRAMANIYAN, S. P., IMAM, M. A., & PRABHAKAR, P. (2020). Effect of Fiber Packing on Moisture Diffusivity and Tortuosity in Fiber Reinforced Composites. In *Proceedings of the American Society for Composites—Thirty-fifth Technical Conference*.
6. Dörr, A., Sadiki, A., & Mehdizadeh, A. (2013). A discrete model for the apparent viscosity of polydisperse suspensions including maximum packing fraction. *Journal of Rheology*, 57(3), 743-765.
7. Cheng, G. J., & Yu, A. B. (2013). Particle scale evaluation of the effective thermal conductivity from the structure of a packed bed: radiation heat transfer. *Industrial & engineering chemistry research*, 52(34), 12202-12211.
8. Guo, B. Y., Yang, S. Y., Xing, M., Dong, K. J., Yu, A. B., & Guo, J. (2013). Toward the development of an integrated multiscale model for electrostatic precipitation. *Industrial & Engineering Chemistry Research*, 52(33), 11282-11293.
9. An, X., Yang, R., Dong, K., & Yu, A. (2011). DEM study of crystallization of monosized spheres under mechanical vibrations. *Computer Physics Communications*, 182(9), 1989-1994.
10. Yi, L. Y., Dong, K. J., Zou, R. P., & Yu, A. B. (2011). Coordination number of the packing of ternary mixtures of spheres: DEM simulations versus measurements. *Industrial & engineering chemistry research*, 50(14), 8773-8785.
11. Zou, R. P., & Yu, A. B. (1996). Evaluation of the packing characteristics of mono-sized non-spherical particles. *Powder technology*, 88(1), 71-79.
12. Donev, A., Cisse, I., Sachs, D., Variano, E. A., Stillinger, F. H., Connelly, R., ... & Chaikin, P. M. (2004). Improving the density of jammed disordered packings using ellipsoids. *Science*, 303(5660), 990-993
13. Zhao, B., An, X., Wang, Y., Zhao, H., Shen, L., Sun, X., & Zou, R. (2020). Packing of different shaped tetrahedral particles: DEM simulation and experimental study. *Powder Technology*, 360, 21-32.
14. Cundall, P. A., & Strack, O. D. (1979). A discrete numerical model for granular assemblies. *geotechnique*, 29(1), 47-65.
15. Rahman, A., & Stillinger, F. H. (1971). Molecular dynamics study of liquid water. *The Journal of Chemical Physics*, 55(7), 3336-3359.
16. Wu, C. Y. (2012). Discrete element modelling of particulate media. *Royal Society of Chemistry*
17. Soltanbeigi, B., Podlozhnyuk, A., Papanicolopoulos, S. A., Kloss, C., Pirker, S., & Ooi, J. Y. (2018). DEM study of mechanical characteristics of multi-spherical and superquadric particles at micro and macro scales. *Powder Technology*, 329, 288-303.

18. Barr AH (1981) Superquadrics and angle-preserving transformations. *IEEE Comput Graph Appl* 1(1):11–23. doi:10.1109/MCG.1981.1673799
19. Podlozhnyuk, A., Pirker, S., & Kloss, C. (2017). Efficient implementation of superquadric particles in Discrete Element Method within an open-source framework. *Computational Particle Mechanics*, 4(1), 101-118.
20. --Gan, J. Q., Zhou, Z. Y., & Yu, A. B. (2018). Structure analysis on the packing of ellipsoids under one-dimensional vibration and periodic boundary conditions. *Powder Technology*, 335, 327-333.
21. Zhao, S., Evans, T. M., & Zhou, X. (2018). Three-dimensional Voronoi analysis of monodisperse ellipsoids during triaxial shear. *Powder Technology*, 323, 323-336.
22. Delaney, G. W., & Cleary, P. W. (2009, June). Fundamental relations between particle shape and the properties of granular packings. In *AIP Conference Proceedings* (Vol. 1145, No. 1, pp. 837-840). American Institute of Physics.
23. Dong, K., Wang, C., & Yu, A. (2016). Voronoi analysis of the packings of non-spherical particles. *Chemical Engineering Science*, 153, 330-343.
24. Pereira, G. G., & Cleary, P. W. (2017). Segregation due to particle shape of a granular mixture in a slowly rotating tumbler. *Granular Matter*, 19(2), 23.
25. Wang, S., Wang, S., & Chen, H. (2019). Numerical influence analysis of the packing structure on ceramic breeder pebble beds. *Fusion Engineering and Design*, 140, 41-47.
26. Cabiscol, R., Finke, J. H., & Kwade, A. (2018). Calibration and interpretation of DEM parameters for simulations of cylindrical tablets with multi-sphere approach. *Powder Technology*, 327, 232-245.
27. Ferrero, M. (2011). Voronoi diagram: The generator recognition problem. arXiv preprint arXiv:1105.4246.
28. Poupon, A. (2004). Voronoi and Voronoi-related tessellations in studies of protein structure and interaction. *Current opinion in structural biology*, 14(2), 233-241. DOI: 10.1016/j.sbi.2004.03.010
29. Moctezuma, R. E., Arauz-Lara, J. L., & Donado, F. (2018). Structural characterization of a magnetic granular system under a time-dependent magnetic field: Voronoi tessellation and multifractal analysis. *Physica A: Statistical Mechanics and its Applications*, 496, 27-39. DOI: 10.1016/j.physa.2017.12.123
30. Andronov, L., Michalon, J., Ouararhni, K., Orlov, I., Hamiche, A., Vonesch, J. L., & Klaholz, B. P. (2018). 3DClusterViSu: 3D clustering analysis of super-resolution microscopy data by 3D Voronoi tessellations. *Bioinformatics*, 34(17), 3004-3012. doi: 10.1093/bioinformatics/bty200
31. Luchnikov, V., Medvedev, N., & Sampson, W. (2006, July). Voronoi modelling of the void structure in three dimensional and near-planar random fibre networks. In *2006 3rd International Symposium on Voronoi Diagrams in Science and Engineering* (pp. 241-245). IEEE.
32. Kloss, C., Goniva, C., Hager, A., Amberger, S., & Pirker, S. (2012). Models, algorithms and validation for opensource DEM and CFD–DEM. *Progress in Computational Fluid Dynamics, an International Journal*, 12(2-3), 140-152. <https://www.aspherix-dem.com/>
33. Ayachit U 2015 *The paraview guide: a parallel visualization application*. Kitware, Inc.
34. Schneider C A, Rasband W S and Eliceiri K W 2012 *Nat. Methods* 9 671
35. Campello EMB (2015) A description of rotations for DEM models of particle systems. *Comput Part Mech* 2(2):109–125. doi:10.1007/s40571-015-0041-z, <http://link.springer.com/10.1007/s40571-015-0041-z>

36. Nassar A I, Thom N and Parry T 2016 *Constr. Build. Mater.* 104 216
37. Kim M J, Kim S, Yoo D Y and Shin H O 2018 *Constr. Build. Mater.* 178 233

Appendices

Appendix A. Running files sample for PySetVoronoi

Test.py file:

```

import sys,os,os.path
sys.path.insert(1, '../install/lib')

import setvoronoi as sv
#print cf.__doc__
mycf = sv.CellFactory()
mycf.infolder = "./input"
mycf.outfolder = "./output"
mycf.posFile = "./Particles.dat"
mycf.wallFile = "./Walls.dat"
mycf.cellVTK = True
mycf.cellPOV = True
mycf.threadNum = 2
mycf.scale = 1000
mycf.boxScale = 3.0
mycf.parShrink = 0.1e-3
mycf.searchRadius = 4.0
#you can execute it step by step
mycf.genPointClouds(w_slices=50,h_slices=40)#here you can put your raw
data
mycf.neighborSearch()
mycf.processing()#processing all particles
pid = 0
#mycf.processingOne(pid)#processing only one particle with id of pid
#or you can conduct an automatic work flow
#mycf.autoWorkFlow()

```

Wall.data file (Simulation 1 for pills):

```
4.73536272E-03  0.000000e+00  0.000000e+00
```

```

0.2971664970.000000e+00    0.000000e+00
0.000000e+00    4.72844997E-03    0.000000e+00
0.000000e+00    0.2971500160.000000e+00
0.000000e+00    0.000000e+00    4.58465004E-03
0.000000e+00    0.000000e+00    0.338277012

```

Particles.data file (Simulation 1 for pills of 10 particles):

```

#rx  ry  rz  eps1  eps2  x  y  z  q0  q1  q2  q3
1.00E-02  4.00E-03  4.00E-03  0.6667  0.6667  4.17E-02
      5.06E-03  9.11E-03  -3.70E-02  -0.853246987  0.161277995-
0.494563013
1.00E-02  4.00E-03  4.00E-03  0.6667  0.6667  5.40E-02
      1.15E-02  1.12E-02  -0.581838012  0.5965870020.382470012-
0.399080008
1.00E-02  4.00E-03  4.00E-03  0.6667  0.6667  6.91E-02
      1.20E-02  1.13E-02  5.01E-02  -1.02E-02  -2.48E-02
0.998382986
1.00E-02  4.00E-03  4.00E-03  0.6667  0.6667  0.109255999
      8.81E-03  1.18E-02  -0.384597987  -0.225833997  -
0.541275978-0.712813973
1.00E-02  4.00E-03  4.00E-03  0.6667  0.6667  0.124730997
      1.23E-02  1.14E-02  0.1427340060.164037004-0.691121995  -
0.689252973
1.00E-02  4.00E-03  4.00E-03  0.6667  0.6667  0.140725002
      6.47E-03  1.19E-02  0.1625570060.1703449930.598342001
0.765861988
1.00E-02  4.00E-03  4.00E-03  0.6667  0.6667  0.149511993
      1.10E-02  1.13E-02  0.734295011-0.636143982  0.128810003-
0.198847994
1.00E-02  4.00E-03  4.00E-03  0.6667  0.6667  0.174559996
      1.14E-02  7.21E-03  -0.44126001 -0.659713984  0.199103996
0.574826002

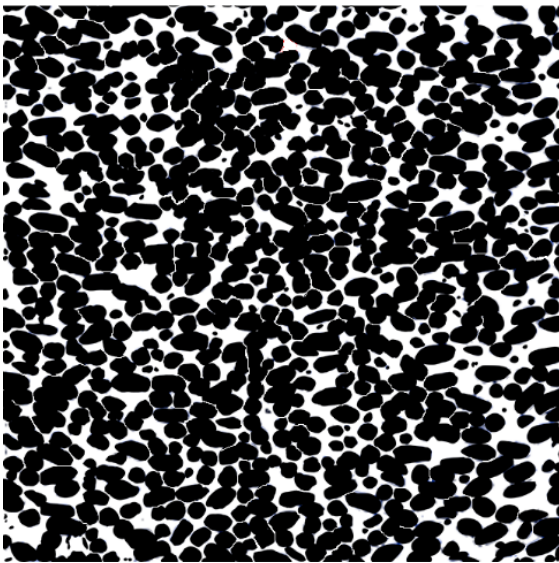
```

1.00E-02 4.00E-03 4.00E-03 0.6667 0.6667 0.235092998
9.62E-03 1.14E-02 0.6554589870.1657219980.450801998
0.582826972

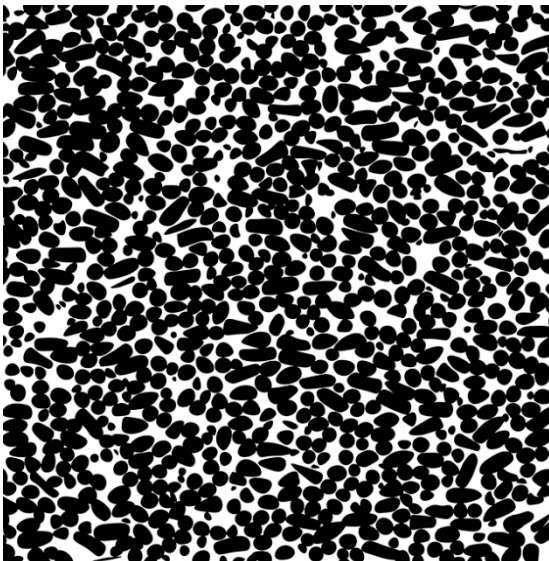
Appendix B. Colored cross sectional images of pills, cylinders and spheres

Normal to Y direction

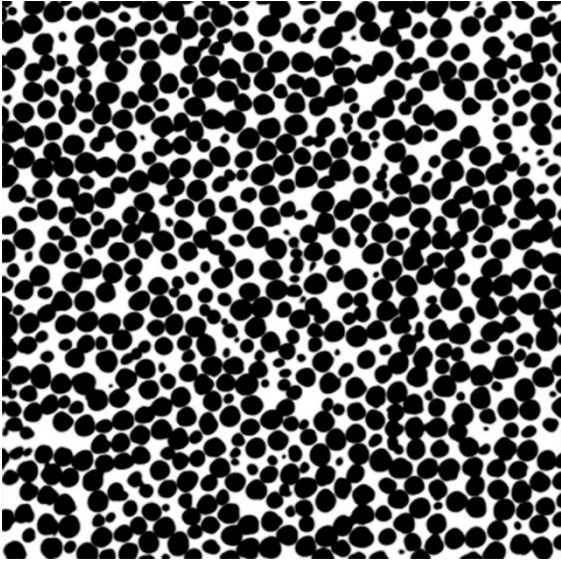
Pills



Cylinders

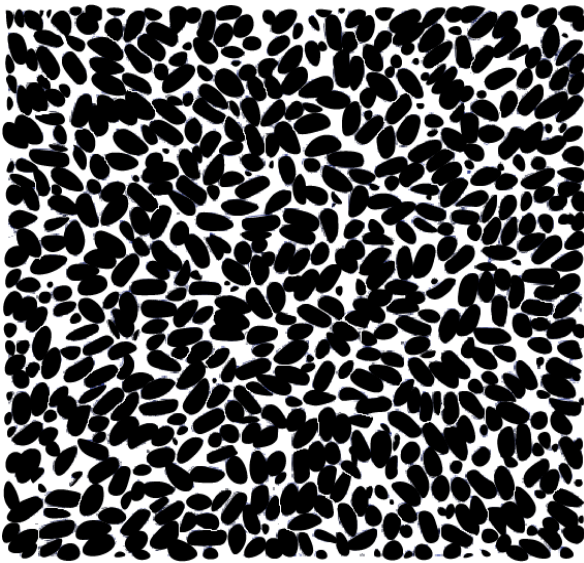


Spheres

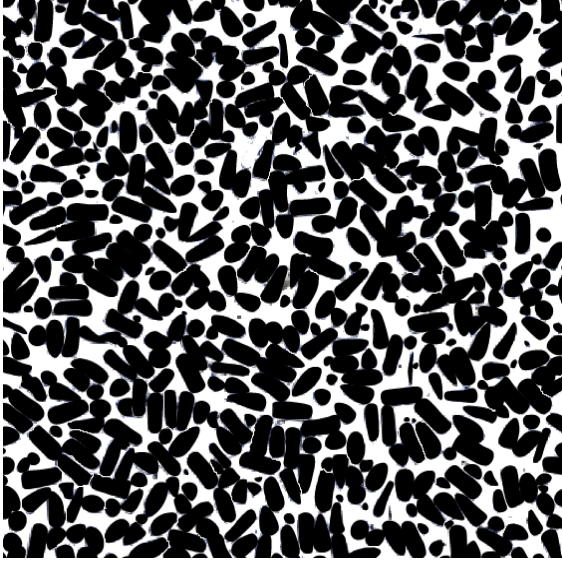


Normal to Z direction

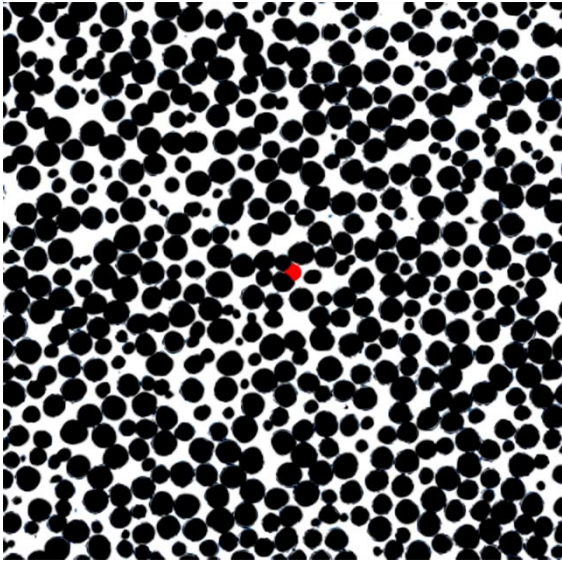
Pills



Cylinders



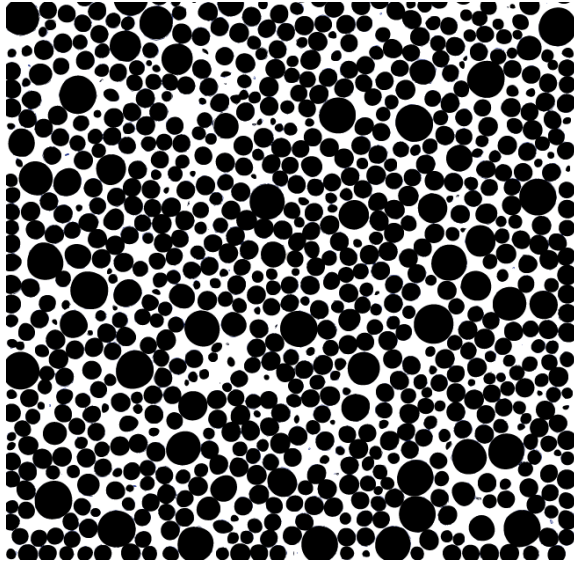
Spheres



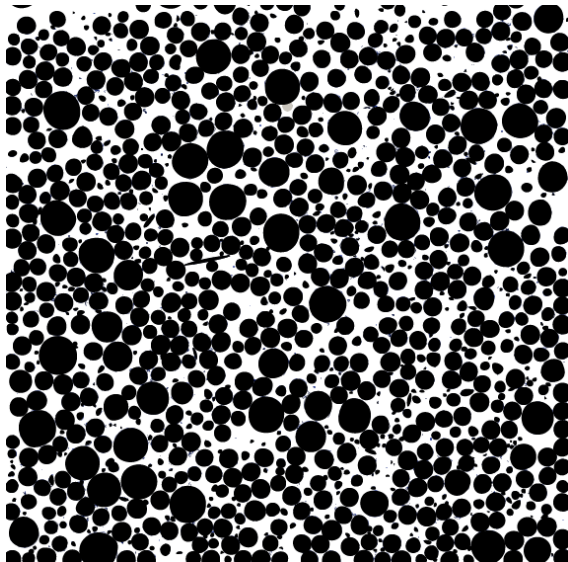
Appendix C. Colored cross-sectional images of binary mixtures
with fibers

Normal to X direction

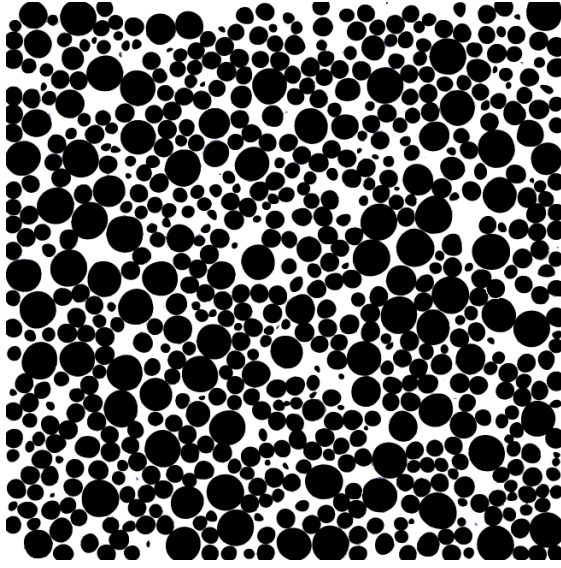
*f*_{fine}:*f*_{coarse}:*f*_{fiber} 62:37:0



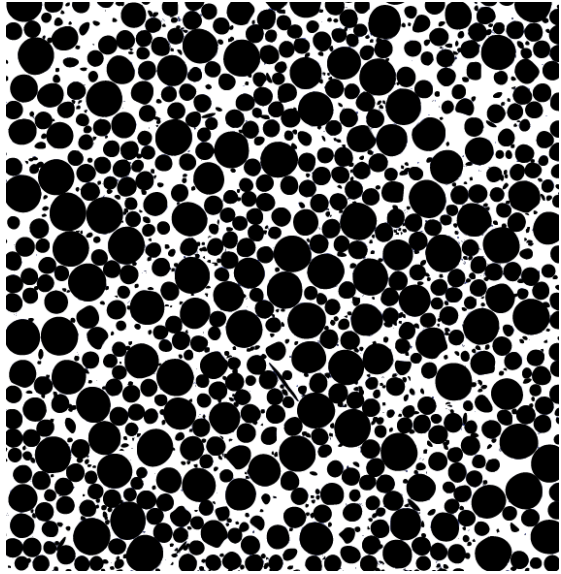
*f*_{fine}:*f*_{coarse}:*f*_{fiber} 62:37:1



*f*_{fine}:*f*_{coarse}:*f*_{fiber} 40:60:0

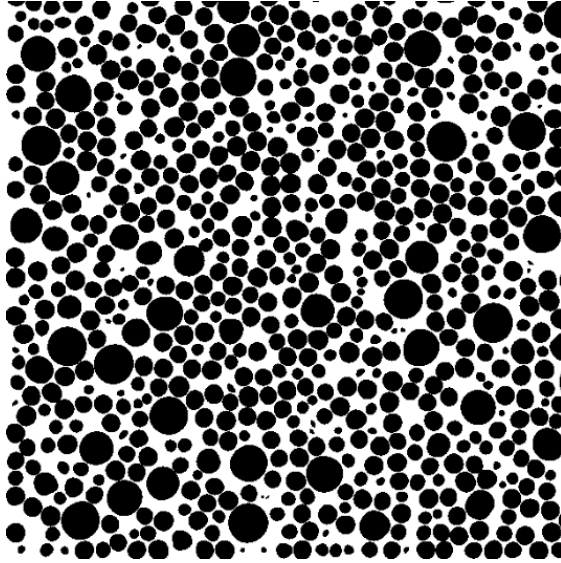


*f*_{fine}:*f*_{coarse}:*f*_{fiber} 40:60:1

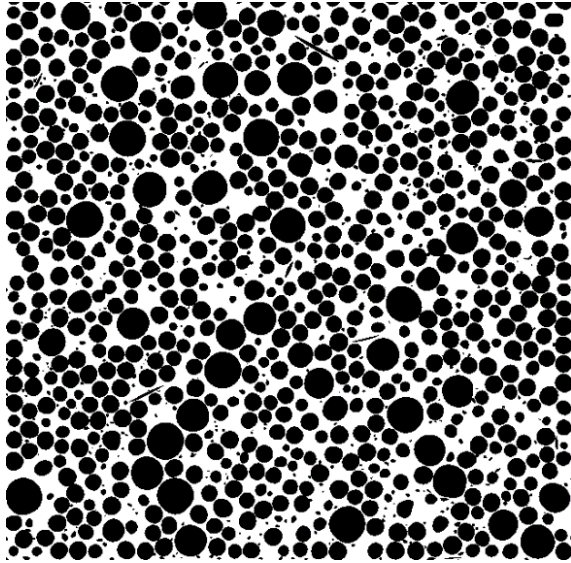


Normal to Y direction

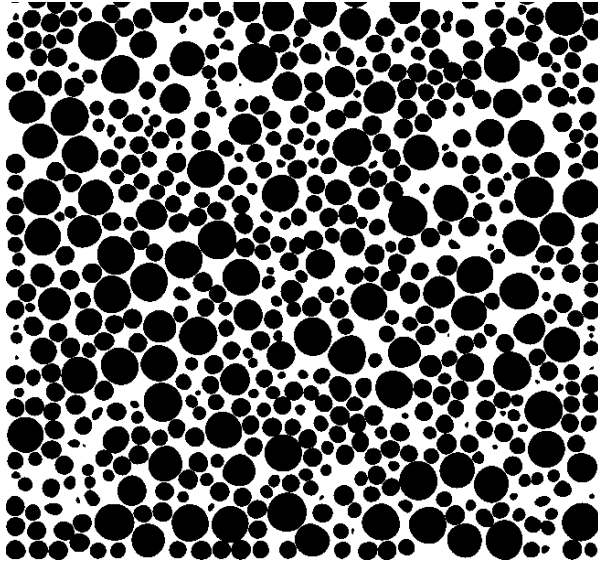
*f*_{fine}:*f*_{coarse}:*f*_{fiber} 62:37:0



*f*_{fine}:*f*_{coarse}:*f*_{fiber} 62:37:1



$f_{fine}:f_{coarse}:f_{fiber}$ 40:60:0



$f_{fine}:f_{coarse}:f_{fiber}$ 40:59:1

